Title
Functional Characterization of EAAT1 Mutations

Author
Mamsa, Hafsa

Publication Date
2017

Peer reviewed|Thesis/dissertation

UNIVERSITY OF CALIFORNIA

Los Angeles

Functional Characterization of EAAT1 Mutations

A thesis submitted in partial satisfaction

of the requirements for the degree Master of Science

in Physiological Sciences

by

Hafsa Mamsa

2017

ABSTRACT OF THE THESIS

Functional Characterization of EAAT1 Mutations

by

Hafsa Mamsa

Master of Science in Physiological Science

University of California, Los Angeles, 2017

Professor Mark Arthur Frye, Co-Chair

Professor Joanna C. Jen, Co-Chair

Episodic ataxias (EAs) are clinically and genetically heterogeneous conditions manifesting with intermittent and recurrent attacks of incoordination and imbalance triggered by stress and exertion. Advances in sequencing have led to the identification of an increasing number of genetic variants of unknown significance. EA6 was designated based on the discovery of a spontaneous heterozygous mutation in a child with EA in *SLC1A3*, which encodes a glial glutamate transporter, EAAT1. The focus of my thesis is twofold: to ascertain potential pathogenicity of two new genetic variants in *SLC1A3*, and to generate and validate transgenic fruit flies as a model organism for EA6. I present data demonstrating impaired glutamate uptake of the mutant transporters in expression studies in both mammalian and insect cell lines to support pathogenicity of the two genetic variants. Furthermore, I generated transgenic fruit flies

that harbor the first human EA6 mutation and found the mutant fruit flies with markedly decreased survival, which could be used in future studies to screen for drug response and modifier genes.

The thesis of Hafsa Mamsa is approved.

Rachelle Hope Watson

Mark Arthur Frye, Committee Co-Chair

Joanna C. Jen, Committee Co-Chair

University of California, Los Angeles

2017

TABLE OF CONTENTS

LIST OF FIGURES

CHAPTER 1 : INTRODUCTION

Episodic ataxias (EAs) are prototypical neurological channelopathies characterized by paroxysmal attacks of incoordination and imbalance typically triggered by emotional stress and physical exertion. EA1 caused by mutations in *KCNA1* encoding a neuronal voltage-gated potassium channel and EA2 caused by mutations in *CACNA1A* encoding a neuronal voltage-gated calcium channel are the most common and the best understood, yet the genetic causes in the majority of EA patients remain unknown, suggesting genetic heterogeneity with novel genes yet to be identified.

EA6 was designated based on the discovery of a *de novo* mutation in *SLC1A3* that encodes a glial glutamate transporter EAAT1 in a child with episodic ataxia and other neurological manifestations including hemiplegic migraine, epilepsy, and progressive ataxia with cerebellar atrophy. The focus of my thesis is twofold: to ascertain potential pathogenicity of two new genetic variants in *SLC1A3* (Chapter 2), and to generate and validate transgenic fruit flies as a model organism for EA6 (Chapter 3). In Chapter 4 I summarize and discuss my findings.

Primary episodic ataxias are clinically and genetically heterogeneous.

The clinical hallmark of EA is intermittent recurrent attacks of imbalance and incoordination triggered by exertion and stress. Heterogeneity in the clinical signs and symptoms not only exist between the different EA subtypes but also amongst affected members within kindreds. Several associated symptoms may occur during an attack, such as vertigo (room spinning dizziness), headaches, weakness, epilepsy, tinnitus, visual disturbances, and hemiplegia (one-sided weakness or paralysis). There is also variation in the common triggers, frequency of

attacks, duration, and age of onset. Between attacks, patients may feel normal or may suffer interictal symptoms. Online Mendelian Inheritance in Man (OMIM) currently lists 8 genetic loci for episodic ataxias (EA1-8) [1]. The most common and best characterized are EA1 and EA2. Both sporadic and familial cases have been reported. When there is a clear family history, an autosomal dominant transmission is evident, and heterozygous mutations have been identified. EA6 caused by mutations in *SLC1A3* is the focus of this thesis. Below I briefly describe the other known EA subtypes and related conditions including familial hemiplegic migraine (FHM) subtypes 1-3, with known genes that include ion channels and ion pumps that are important in regulating neuronal excitability and neurotransmission.

Mutations in KCNA1 and CACNA1A are the major cause episodic ataxia.

The first EA gene: EA1

EA1 is an autosomal dominant disorder affecting both the central and peripheral nervous system characterized by bouts of ataxia lasting seconds to minutes and interictal myokymia (fine muscle rippling) [2]. The most common symptoms during attacks are imbalance, incoordination, and dysarthria, and weakness [3]. Epilepsy is more prevalent than expected [4]. Attacks may occur spontaneously but often triggered by physical exertion, emotional stress, sudden abrupt movements, startle, [3]. Symptoms begin early in childhood. Acetazolamide and carbamazepine occasionally help alleviate symptoms. The worldwide disease prevalence is roughly estimated at 1:500,000 [5].

Mutations in the causative gene, *KCNA1*, with a single coding exon were first discovered by Browne and colleagues after performing linkage analysis [6] and candidate gene sequencing in four unrelated families with ataxia and myokymia [7]. This was the first report implicating a

potassium channel gene in human disease, and this was also the first report of a channelopathy with central nervous system manifestations. *KCNA1* encodes the voltage gated Kv1.1 potassium channel homologous to the fruit fly *Shaker* potassium channel important in repolarization. At least 29 missense mutations, a single in-frame deletion and a single truncation mutation have been identified thus far [5]. *In vitro* studies demonstrate that most of these mutation alter channel function or protein expression [8].

EA2

Autosomal dominant episodic ataxia type 2 (EA2) is the most common form of EA. It is characterized by paroxysmal attacks of ataxia lasting hours with interictal nystagmus and mild baseline ataxia [9, 10]. Attacks usually begin before age 20 but later onset has also been reported [11]. Variably associated symptoms can include vertigo, nausea, vomiting and migraine. Symptoms are often alleviated by acetazolamide.

EA2 is caused by mutations in *CACNA1A*, which encodes the pore-forming and voltage-sensing subunit of Cav2.1, the P/Q type voltage gated calcium channels that is abundantly expressed in the cerebellum and at the neuromuscular junction as the major presynaptic voltage-gated calcium channel that mediates neurotransmission [12, 13]. *CACNA1A* with approximately 50 exons spanning 300,000 bases is extensively alternative spliced. Different heterozygous mutations in the same gene have also been identified in individuals and families with hemiplegic migraine commonly associated with interictal nystagmus and progressive ataxia, which is designated FHM1 (OMIM 141500) [1, 13]. Furthermore, expansion of a polymorphic glutamine-encoding CAG repeats in *CACNA1A* causes spinocerebellar ataxia type 6 (SCA6) [14]. More than 50 mutations have been reported in EA2, most of which are splice site or nonsense mutations that likely result in a truncated protein [15, 16], while FHM1 is more

commonly linked to missense mutations in the same gene. Large multi-exonic deletions not detectable by routine sequencing have also been identified in rare cases [17, 18].

The other EAs defined by single families:

EA3

EA3 was described by Steckley and colleagues in a single Canadian kindred with episodic ataxia and vertigo [19]. Seventeen of the 25 affected individuals had tinnitus during these episodes. Many individuals also reported visual disturbances (visual blurring, diplopia) and (migraine-like) headache reminiscent of migraine with aura. Fatigue, stress, physical exertion, and head movements triggered the attacks. Attacks typically lasted less than 30 min. There was a positive response to Acetazolamide. Linkage analysis mapped the disease locus to a 4cM region on 1q42 but a causative gene has yet to be reported [20].

EA4

EA4, also known as periodic vestibulocerebellar ataxia, was reported in two families from North Carolina [21, 22]. Attacks were characterized by episodes of vertigo, ataxia, diplopia and interictal nystagmus. The age of onset ranged from 23-60 years. Attacks typically lasted minutes to hours but could also occur for weeks to months. Common triggers were fatigue, abrupt head movements, or watching moving objects. There was no response to Acetazolamide. The EA1 and EA2 loci along with SCA 1-5 were ruled out by combined linkage analysis of both families [22]. No disease locus has been reported.

EA5

While screening a cohort of families with epilepsy or ataxia for mutations in *CACNB4*, which encodes the calcium channel B4 subunit, an auxiliary subunit of Cav2.1, Escayg et al found a heterozygous missense variant (c.311 G>T, p.C104F) in 5 affected and 2 asymptomatic individuals of a French Canadian family. The family presented with episodes of ataxia and vertigo similar to EA2 but no mutation was found in *CACNA1A*. The identical variant was found in a German family with generalized epilepsy but no ataxia. Functional in vitro studies in *Xenopus laevis* oocytes showed only mild changes in calcium channel current density. A search of recently available exome sequencing data reports this variant occurs in 45 of 60,006 individuals at an allele frequency of 0.045% in the general population [23]. The higher than expected allele frequency for a rare condition such as episodic ataxia, that the identical variant was found in multiple individuals, and that since the original report was published in 2000 no other variants in *CACNB4* have been identified in EA or epilepsy patients, raise concerns that this variant may not be pathogenic.

EA7

EA7 was described in a single family in which all seven affected members had very similar attacks of ataxia, weakness, and dysarthria triggered by exercise or excitement with onset before the age of 20 [24]. Two individuals also presented with vertigo. There were no interictal symptoms. Genome wide linkage analysis mapped the disease locus to a 10cM region on 19q13. The causal gene has not been identified.

EA8

The newest reported EA was found in a single Irish family with thirteen affected individuals presenting with attacks of unsteady gait, generalized weakness and slurred speech with infantile onset triggered by stress and fatigue [25]. Patients experience mild intention tremor, gait ataxia, and dysarthria in between attacks. Some individuals had gaze evoked nystagmus. Linkage analysis identified a 18.5 Mb locus at 1p36.13-p34.3. Exome sequencing analysis within the linkage region identified two potential causative variants HSPG2 (S2380R) and URB4 (R5091H). No mutations were found in known EA genes. Authors suggested UBR4, a ubiquitin-protein ligase, as a likely candidate and hypothesized its role in calcium signaling. No functional characterization was reported and this variant remains of unknown significance.

CACNA1A: A link between EA, FHM, and SCA

The disease locus for EA2 and a subset of families with familial hemiplegic migraine (FHM) mapped to the identical locus on 19p13 [26-28]. *CACNA1A* was simultaneous reported as the causative gene for both EA2 and FHM1 [13]. Soon thereafter, abnormal glutamine coding CAG repeat expansions at the C-terminal end of *CACNA1A* was found to cause late onset spinocerebellar ataxia type 6 (SCA6) [14]. Therefore, EA2, FHM2, and SCA6 are allelic disorders arising from mutations in the identical genes with distinct clinical manifestations but overlapping symptoms and signs.

Familial Hemiplegic Migraine is also phenotypically and genotypically heterogeneous

Migraine is clinically defined by migraine without aura (MO) and migraine with aura (MA). Migraine is estimated to affect 15% of the general population; 25% of those with migraine has aura [29]. Familial hemiplegic migraine is a rare subtype of migraine in which the

migraine episodes are accompanied by complicated aura manifesting with unilateral weakness or numbness. A key distinguishing symptom (from MA) is the presence of transient motor involvement in FHM which manifests as transient mild hemiparesis (weakness) or paralysis (hemiplegia) and usually involves a limb or one side of the body [8, 30]. The hemiparesis is accompanied by at least one other neurological aura symptom such as visual disturbance, sensory loss, and/or dysphasia (difficulty formulating or comprehending speech) [30]. The aura usually begins before onset of the headache, typically lasts for hours but can be prolonged for days and can outlast the migraine headache. Variably associated symptoms are confusion, coma, and seizures [31-33]. Attacks can be triggered by stress, trauma, exertion, foods, odors, and bright light [34] with onset usually within the first two decades . There have also been reports of long attack free intervals ranging from 2-37 years or attack free intervals of as long 37 years between attacks [32]. There are currently three known loci for FHM that I briefly discuss below.

FHM1 caused by mutations in CACNA1A

A key distinguishing factor for FHM1 is a higher frequency of cerebellar signs and symptoms in addition to hemiplegic episodes. In some patients, episodic ataxia and hemiplegic migraine can occur simultaneously [32, 35]. In a study conducted by Ducros and colleagues in a cohort of 117 FHM participants who harbored mutations in *CACNA1A*, 60% of patients had permeant cerebellar signs of nystagmus (most frequent), ataxia, and/or dysarthria [32]. Cerebellar atrophy has been reported in 25% of individuals 10% of individuals show no symptoms of hemiplegia but have migraine with or without aura [32].

FHM2 caused by mutations in ATP1A2

Soon after the discovery of FHM1, mutations in *ATP1A2* were linked to FHM2 [36]. *ATP1A2* encodes the alpha2 catalytic subunit of the sodium-potassium ATPase pump expressed predominantly in glia. This protein derives energy from ATP to actively transport sodium ions out and potassium ions into cell. This mechanism maintains the electrochemical gradient and the resting membrane potential that is essential for the function of ion channels and transporters in the cell membrane.

FHM2 accounts for the greatest number of hemiplegic migraine cases linked to a disease gene and at least 60 mutations (mostly missense) scattered throughout the gene have been reported for both familial and sporadic cases [29]. Seizures may be more prevalent compared to FHM1 [31, 36, 37]. Of note, rare patients with cerebellar signs have been reported [31, 37, 38].

FHM3: SCN1A

There is clearly a higher incidence of seizures in FHM patients compared to the general population [29]. The key link came when Dichgans and colleagues identified an identical missense mutation in three families with FHM3 in *SCN1A*, a gene well associated two types of epilepsy (Generalized epilepsy with febrile seizures plus and Dravet syndrome) [39]. The genotype co-segregated with the phenotype in all three families. Several mutations have been identified thereafter with or without co-occurrence of epilepsy [39-45]. *SCN1A* encodes the pore-forming alpha 1 subunit of the neuronal voltage gated sodium channel Nav1.1, important for generation and propagation of action potentials.

Alternating hemiplegia of childhood

Alternating hemiplegia of childhood (AHC) is neurodevelopmental disorder with a very early or infantile onset in which patients experience paroxysmal spells of hemiplegia or hemiparesis on one or both sides of the body. In between attacks patients may manifest some combination of persistent neurological impairment such as developmental delay, cognitive impairment/intellectual disability, behavioral problems, and motor impairments, such as choreoathetosis, dystonia, ataxia, hypotonia or oculomotor apraxia. Epileptic seizures are common in 40-50% of patients [46, 47]. Episodes could occur for minutes but can last as long as a few weeks [46]. Common triggers include environmental, physical or emotional stress [46]. Two genes have been implicated in AHC: *CACNA1A* and *ATP1A3*.

AHC is allelic to FHM2: ATP1A2

In 2004 Bassi et al first reported a mutation that co-segregated in 4 affected members of a family with alternating hemiplegia of childhood [48]. Although only a handful of cases with *de novo* mutations in this gene have been identified [48, 49]. Swoboda identified the identical mutation in a second family with AHC and only mild intellectual disability in patients with overlapping FHM and AHC clinical features [49].

AHC2 due to mutation in ATP1A3

More recently, *ATP1A3* was identified to be the predominant cause of AHC [50]. In a cohort of 105 unrelated cases, Heinzen et al identified a total of 19 different mutations in 82 cases. Most mutations were missense, a single splice site, and another deletion likely altering the open reading frame of the protein. In at least 59 cases for which the parental DNA was available, the mutation was shown to arise *de novo*, suggesting hotspots for mutations. The

percent of AHC cases with *ATP1A3* mutation ranges from 74-85% in two large cohorts [50, 51]. Interestingly, a handful of mutations cause either AHC in some patients and rapid onset dystonia and parkinsonism in other patients.

AHC3 due to mutation CACNA1A in a single case

A *de novo* variant in *CACNA1A* was identified in two monozygotic twins presenting with overlapping features of both FHM (hemiplegia with migraine headaches and aura) and atypical AHC with a later age of onset (early-onset ataxia, alternating hemiplegia, epilepsy, migraine with aura, and intellectual disability) [52].

Aims

In chapter 2, I review the functional studies on the first EA6 mutation and investigate the functional consequences of two novel variants identified in EAAT1.

In chapter 3, I create and validate a *Drosophila melanogaster* model of EA6.

CHAPTER 2 : FUNCTIONAL CONSEQUENCES OF EAAT1 MUTATIONS *IN VITRO*

Introduction

Episodic Ataxia Type 6: clinical and genetic features

Case 1. c.869C>G; Pro290Arg in episodic and progressive ataxia, hemiplegic migraine, epilepsy designated EA6

The first pathogenic mutation in *SLC1A3* was discovered in a 6 year old boy with episodic ataxia, progressive ataxia, hemiplegic migraine, epilepsy, and mild cerebellar atrophy [53]. This *de novo* mutation, c.869 C>G in *SLC1A3*, was predicted to lead to the substitution of arginine for a proline (p.P290R) that is evolutionarily conserved from bacteria to human (Figure 2-1)[53]. *In vitro* studies demonstrated profoundly reduced protein expression and glutamate uptake activity (which I performed) by the mutant EAAT1-P290R compared to wildtype EAAT1 (Figure 2-2, 2-3)[53]. Furthermore, co-expression of wildtype and mutant EAAT1 showed a dominant negative effect of the mutant on wildtype protein expression and glutamate uptake function (Figure 2-2, 2-3)[53].

Subsequently 2 additional mutations in *SLC1A3* were identified in two unrelated families with overlapping clinical features with the first index patient.

Case 2. c.556T>A; p.Cys186Ser in episodic ataxia and migraine without aura

Also by a candidate gene approach, a heterozygous variant s c.556 T>A; p.C186S was identified in a Dutch family with pure episodic ataxia and no disease causing mutations in known causative EA genes (Figure 2-4). The variant appeared to segregate with the phenotype in this small pedigree, as it was present in the proband's affected mother and sister, along with a cousin

with migraine without aura (but no episodic ataxia) but absent in a second asymptomatic cousin. (Figure 2-5) The genetic variant appeared to be rare, since it was not present in 200 ethnically matched control samples. C186 resides in the fourth transmembrane domain of EAAT1. This residue is conserved from zebrafish to human.

Case 3. c.1159A>C p.T397P in migraine with and without hemiplegia

SLC1A3 was interrogated for mutations in a proband with numerous hemiplegic migraine attacks beginning at the age of 11, but in whom no mutations were identified in known FHM genes [54]. Sanger sequencing revealed a heterozygous missense mutation c.1159A>C p.T397P. The resulting protein has a proline substituted for a threonine residue conserved from worms to humans (Figure 2-4). His father, who has migraine without aura, also harbors the variant. The mutation was not found in 50 ethnically matched control individuals.

EAAT1- structure and function

Glutamate is the most abundant excitatory neurotransmitter in the mammalian central nervous system [55]. Regulating spatial and temporal levels of extrasynaptic glutamate is crucial in regulating function of glutamatergic synapses, preventing hyperexcitability and neuronal cell death [56]. Glutamate excitotoxicity has been implicated in several neurological disorders such as stroke, epilepsy, ischemia, Alzheimer's, and Amyotrophic lateral sclerosis [57]. Glutamate transporters are responsible for clearing glutamate from the synaptic cleft during neural transmission.

There are at least five glutamate transporter subtypes, EAAT 1-5, and two neutral amino acid transporters (ACST1 and ACST2), each with a distinct distribution in the CNS [58-60]. Although EAAT1 is expressed throughout the CNS it is primarily expressed in the diencephalon,

caudal brainstem, and most abundantly in the cerebellum [59, 61]. Two glial glutamate transporters exist in vertebrates: EAAT1 (or GLAST) and EAAT2 (or GLT1) [62]. In the rat cerebellum, EAAT1 is expressed at six fold greater levels than EAAT2 [63]. The other EAATs are expressed in neurons.

No crystal structure exists for any of the vertebrate EAATs. In recent years, several crystal structures have been published for an orthologus bacterial glutamate transporter homologue, Gltph, from *Pyrococcus horkoshii*, which shares 28% amino acid identity and 42% amino acid similarity to human EAAT1 [64-66]. Glutamate transporters assemble as a trimeric complex [67, 68]. Each transporter is composed of eight alpha-helix transmembrane domains (TM 1-8) and two reentrant hairpin loops (HP1 and HP2 formed be helix-turn-helix motif) (Figure 2-4) [64]. N-terminal transmembrane domains 1-6 forms inter-subunit contacts with TM2, TM4, and TM5 constituting the interaction surface between promoters or trimerization motif. This forms a wedge shaped scaffold that cradles and stabilizes a compact C-terminal transport domain, composed of TM7, HP1, HP2 and TM8 that constitutes substrate binding site. The transport domain undergoes large conformational changes during the transport cycle. It also serves as the binding site for glutamate and coupled ions (Na+, H+, K+). HP1 and HP2 have been hypothesized to form the internal and external gates.

Within this trimeric complex, each monomer can function independently. Glutamate transporters couple the influx of a single glutamate with three sodium and one hydrogen ion into the cell with the outward counter transport of one potassium ion [57]. More recently, the glutamate transporters have gained greater recognition for their dual function as a anion channel in addition to their role as secondary active glutamate transporters in human and Gltph [57, 69].

To investigate whether and how the genetic variants may alter the function of the gene products, I performed *in vitro* expression studies.

C186S

C186 is located within transmembrane domain segment 4B at the outer perimeter of the promoter [64, 70]. TM4 consists of three segments of a helix-turn-helix-turn-helix and is part of the trimerization domain implicated in inter-subunit interaction[64]. The 4B-4C loop has been reported to have substrate-induced conformational changes [70]. The 4B-4C loop has been postulated to play a role in forming stable trimers and may also be important for coordinating cooperativity of binding of Na+ ions by each promoter within the trimeric structure[70].

T387P

T387 residing in TM7a is part of the substrate binding transport domain [64]. The transport domain undergoes structural changes as ions are bound and translocated across the membrane. Substituting a small threonine residue, with proline, a rigid hydrophobic residue which can form bends in proteins may inhibit conformation changes required for ion binding or translocation. Several residues within TM7 contribute to the glutamate and cotransported ion Na+, K+, H+ [57]. TM7 has also been implicated in anion binding and anion conductance [57, 71].

Materials and Methods

Cloning and Mutagenesis

Mutant constructs were created by site directed mutagenesis of the wild type cDNA in pcDNA3.1/Zeo(+) with QuikChange II XL Site-Directed Mutagenesis Kit (Agilent) according to

manufactures instructions. 2µl of the Dpn I treated reaction was transformed into XL10-Gold ultracompetent cells, plated onto LB-ampicillin agar plates and grown overnight at 37°C. The next day, colonies were inoculated into LB-ampicillin broth and cultured at 37°C with shaking for 14-16 hrs. Plasmid was extracted with the QIAprep Spin Miniprep Kit (Qiagen) according to manufactures instructions. All constructs were bidirectionally sanger sequenced.

COS7 cell culture and transfection

COS-7 cells obtained from American Type Culture Collection (ATCC) were maintained as sub-confluent cultures in Dulbecco's Modified Eagle's Medium (DMEM; Invitrogen) supplemented with 9% fetal bovine serum (FBS; Invitrogen) at 37°C and 5% CO2. One day before transfection, sub-confluent cells were dissociated with 0.25% trypsin-EDTA (Invitrogen) and counted with a hemacytometer. $8x10^5$ cells in culture medium were seeded per well of a 60 mm tissue culture plate and transfected with 8ug construct DNA and Lipofectamine 2000 (Invitrogen) the next day. Culture medium was change five hours later. Cells were cultured until reseeding or harvesting. DNA was kept constant at 8 µg per plate by cotransfecting a carrier plasmid such as pcDNA3.1.

Glutamate uptake assay

One day after transfection onto 60mm tissue culture dish, COS7 cells were dissociated with Enzyme free cells dissociation buffer, plated onto three 60 mm dishes and cultured overnight. The next day, glutamate uptake assay was performed at room temperature. Cells were washed twice with uptake wash buffer (uptake buffer without glutamate) before incubation with 1.5 ml glutamate uptake buffer for 2 min. Glutamate not taken up by the cells was removed by washing twice with uptake wash buffer before lysing cells with 1 ml 0.1% (v/v) Triton-X100. Lysate was spun for 10 min 4°C and the supernatant transferred to a new tube.

500 µl lysate was diluted in 5 or 10 ml of scintillation fluid and the amount of radioactivity measured with a scintillation counter. Protein concentrations were determined using the Micro BCA protein assay kit (Pierce) using bovine serum albumin as a standard. Glutamate uptake was determined by quantifying the pmol glutamate/mg protein/min. Sodium dependence was tested by substituting NaCl with Choline chloride.

Glutamate Uptake Buffer:

25 mM Tris-HCl pH 7.3

125 mM NaCl

4.8 mM KCl

1.3 mM CaCl2

1.2 mM MgSO4

1.2 mM Potassium phosphate buffer [9.1 mM K2HPO4, 2.9 mM KH2PO4]

5.6 mM Glucose

1 µM L-glutamic acid

1 µCi/ml L-[3,4-3H]-glutamic acid

Cell surface protein labeling

48 hours after transfection, COS7 cells cultured on 60 mm dishes were washed three times with ice cold PBS+CaMg. Cell surface proteins were labeled with 3ml of 0.5 mg/ml EZ-Link Sulfo-NHS-SS-Biotin (Pierce Thermo Scientific) in 1x PBS+ for 30 min at 4°C with gentle agitation. Residual biotin was removed with two washes with 100mM Glycine in PBS+ . Remaining non-reacted biotin was quenched by a 30 min incubation in 100mM Glycine in PBS+ at 4°C with gentle agitation. Cells were washed two times with PBS+ before lysing with RIPA buffer containing Halt Protease inhibitors (PI) for 10 min at 4°C with rotation. Cells were

scrapped into a microcentrifuge tube, briefly vortexed and rotated for an additional 20 min on ice. Debri was sediment by centrifuging lysate at 16,000 xg at 4°C for 15 min. and the clarified supernatant was transferred into a new tube. Protein concentration was determined from this total cell protein fraction with the Micro BCA protein assay kit (Pierce). Biotinylated proteins were batch extracted with High Capacity NeutrAvidin Resin was applied to a column and washed with 50mM Tris-PI by centrifugation at 1000 x g for 2 min. The supernatant was discarded and the avidin beads resuspended in 50mM Tris-PI. This mixture was rotated at room temperature for 1 hour. After spinning at 1000 xg for 5 min, beads were washed 4 times with RIPA buffer containing protease inhibitors. Biotinylated membrane proteins bound to avidin were eluted by incubating beads with 1x Nupage sample loading buffer containing 50mM DTT for 1 hour at room temperature before centrifugation for 2 min at 1000 xg. This eluate is the membrane fraction. Protein samples were stored at -80°C. All centrifugation steps were performed at 4°C unless stated otherwise.

Western Blot Analysis

10µg of total cell protein fraction and equimolar amount of the membrane fraction were separated by SDS-PAGE, then transferred onto a nitrocellulose membrane. Western blotting was performed following standard protocols with anti-EAAT1 antibody followed by a secondary antibody horseradish peroxidase conjugated horse anti-mouse IgG (Vector Laboratories; 1:5000). The blot was subsequently stripped and reprobed with chicken anti-GAPDH (Millipore; 1:1000) and secondary antibody horseradish peroxidase conjugated goat anti-Chicken IgY (Abcam; 1:5000). Bound antibodies were visualized with Amersham ECL Plus™ Western Blotting Detection Reagents (Amersham).

Protein Biogenesis and degradation (pulse chase, IP, glycosylation)

COS7 cells cultures in DMEM supplemented with 10% fetal bovine serum (Invitrogen) in 5% CO2 at 37C, Cells in 35 mm wells were transfected with Lipofectamine 2000 using 4 ug of either wildtype or mutant EAAT1 constructs in pcDNA3.1. One day post transfection, cells were dissociated with enzyme free cell dissociation buffer, plated onto three 35mm wells and grown overnight. Cells were washed twice in 1xPBS and starved in cysteine and methionine free DMEM (cellgrow) containing 10% dialyzed FBS for 30 min at 37C. Cells were pulse labeled for 30 min in starve medium containing [35S]cysteine and [35S]methionine and chased in starve medium supplemented with 2mM (each) cysteine and methionine for 5, 10, 24 or 48 hours. Cells were lysed in ice-cold RIPA buffer containing protease inhibitors. Lysates were rotated at 4C for 15 min and centrifuged at 10,000 rpm for 15 min at 4C to remove any insoluble material.

Lysates were pre-cleared using 1 ug normal mouse IgG (Santa Cruz Biotechnology) and protein A/G PLUS agarose beads (Santa Cruz Biotechnology) for 2 hours at 4C with gentle rocking and centrifuged at 10000 rpm for 5 min at 4C to prevent any non-specific binding. The supernatant was incubated overnight with 1ug monoclonal anit-EAAT1 antibody (Novocastra Laboratories) with gentle rocking at 4C, treated with protein A/G PLUS agraose beads for an additional 4 hrs at 4C and centrifuged at 10000 rpm for 2 min at 4C. The pellet was washed four times with ice-cold RIPA buffer for 5 min with gentle rocking at 4C. The final pellet was eluted with 1% SDS and 10x denaturing solution (New England BioLabs) and boiled for 5 min. The resulting supernatant was divided into 3 fractions. Fraction 1 served as a no-treatment control and the remaining two fractions were treated with either PNGase or EndoH (NEB) following manufacturer's instructions at 37C for 2 hrs. Samples were boiled in 4x Laemmeli sample buffer (250mM Tris-HCL pH7.4, 8% SDS, 40% glycerol, and 260 mM DTT) for 5 min, followed by

electrophoresis on 7.5% SDS-PAGE gel (Bio-Rad). Gels were dried at 80C for 1 hr and developed onto phosphoimager.

Results

Do C186S and T387P variants in EAAT1 disrupt glutamate re-uptake?

Glial EAAT1 is responsible for clearing glutamate from the synaptic cleft during neural transmission. To investigate whether the variants C186S and T387P may impair glutamate transport activity, I made wildtype and mutant constructs, which were transiently expressed in COS7 cells. I performed sodium dependent glutamate uptake assays by measuring the amount of internalized radioactive glutamate. Glutamate uptake was profoundly impaired in cells expressing EAAT1-T387P (14.9 ± 0.5) compared to wildtype (57.0 ± 2.2) (Figure 2-6; $p<0.001$). All uptake values are reported as the mean pmol/mg protein/min glutamate incubation. In contrast, there was a modest yet consistent decrease in glutamate uptake by cells expressing EAAT1-C186S (88.2 ± 5.5) versus wildtype (107.8 ± 6.9) (Figure 2-5; $p<0.03$). Mock transfected cells had very little glutamate uptake activity (Figure 2-6).

Glutamate transporters couple the influx of a single glutamate with three sodium and one hydrogen ion into the cell with the outward counter transport of one potassium ion[57]. To test for any alterations in the sodium dependency of glutamate uptake by EAAT1-T387P, I measured glutamate uptake with a modified buffer substituting sodium by choline. There was only residual uptake in the absence of sodium, as cells expressing EAAT1-WT (0.918 ± .081) or EAAT1-T387P (0.955 ± .047) took up glutamate at levels similar to mock transfected control (1.095 ± .066) (Figure 2-6).

Glutamate transporters have been hypothesized assemble as a trimeric complex [67, 68]. To recapitulate the heterozygous state in patients and to investigate whether the mutant allele may interfere with the wildtype allele, glutamate uptake assays were performed on COS7 cells co-transfected with equimolar amounts of wildtype and mutant constructs. Co-expression studies showed that EAAT1-T387P did not have any significant dominant negative effect on wildtype transporter activity as uptake in cells expressing 1 ug each of EAAT1-WT:T387P was 39.9 ± 2.2 and that for 1 ug of WT alone was 38.0 ± 1.6 (Figure 2-6; $p<0.5$).

What are the mechanisms that contribute to reduced glutamate uptake by mutant EAAT1?

The impaired glutamate uptake observed in cells expressing mutant EAAT1 could be due to altered biophysical properties of the transporter, lower protein synthesis or stability, and/or aberrant plasma membrane trafficking. I performed biochemical analysis on transiently transfected COS7 cells to examine the relative stability and plasma membrane localization of mutant EAAT1. Immunoblot analysis of total cell lysates revealed dramatically lower levels of EAAT1-T387P protein compared to wildtype (Figure 2-7). To test for any defects in plasma membrane targeting, residues accessible from the extracellular space were labeled with biotin, enriched with avidin conjugated beads, and probed with anti-EAAT1 antibodies. EAAT1-T387P does indeed localize to the cell surface although at markedly reduced levels compared to wildtype (Figure 2-7). These findings suggest that reduced amounts of total EAAT1-T387P albeit properly targeted to the plasma membrane contributes to the reduced glutamate uptake observed.

EAAT1-P290R undergoes accelerated degradation

In the report describing the first mutation in EAAT1, P290R, the authors showed that the glutamate transport activity in COS7 cells transiently expressing mutant EAAT1 was greatly diminished (Figure 2-2)[53]. Immunoblot analysis of the total cell lysate using anti-EAAT1 antibody indicated that mutant protein is expressed at dramatically lower levels than wildtype (Figure 2-3)[53]. Although the mutant protein was undetectable in the biotinylated plasma membrane fraction, confocal microscopy of immunolabeled cells revealed that despite the decreased overall abundance, at least in some cells, the mutant protein can be targeted to the plasma membrane at levels comparable to wildtype [53].

The reduced levels of mutant protein could be due to lower protein synthesis, increased degradation or both. Pulse chase was performed to further elucidate the mechanism underlying expression and trafficking of EAAT1-P290R. Cells expressing either wildtype or EAAT1-P290R were fed S35- methionine/cysteine to allow newly born proteins to incorporate the radiolabeled residues (this is the pulse phase). After unincorporated label was thoroughly washed away, the cells were immediately harvested or cultured in nonradioactive medium for the indicated time points up to two days (the chase phase). Lysates were immunoprecipitated with anti-EAAT1 antibody, resolved by SDS-PAGE, and radiolabeled protein captured on a phosphoimager. During the initial 30 min pulse labeling, comparable amounts of both wildtype and mutant protein were synthesized and all three, mono-, di-, and trimeric, forms were observed (Figure 2-8, A: lanes 1,3 and B lanes 2,5).

GLAST, the rat homolog of human EAAT1, in addition to other glutamate transporters have been shown to be decorated with N-linked glycans [56, 72]. After 5 hours of chase, higher molecular mass bands were observed for monomers and oligomers for wildtype that were not

present during the first 30 min of pulse while nascent protein was being synthesized (Fig 2-8, lanes 2 vs 8, red filled circles). To examine whether these bands represented different glycosylation states, nascent radiolabeled protein was enriched with anti-EAAT1 antibodies before treatment with Peptide N-Glycosidase F (PNGase F) or Endoglycosidase H (Endo H). PNGase F cleaves most forms of N-linked glycans on Asparagine residues, while Endo H selectively cleaves immature high mannose and some forms of hybrid glycans. Glycosylation begins in the ER and continues as the glycopeptide is trafficked through the Golgi apparatus for further modification. Glycan processing in the medial Golgi shifts the glycans from an immature high mannose state to take the fate of complex oligosaccharides. Resistance to EndoH cleavage is a hallmark of glycopeptides which have passed through the medial Golgi.

Indeed, the higher molecular weight bands observed during the chase periods for wildtype are cleaved by PNGase F but resistant to Endo H (Figure 2-8, B red filled circles), suggesting that these proteins contain more complex oligosaccharides. As the chase time increases, there is a concomitant increase in the amount of mature wildtype glycoprotein relative to the immature forms (Figure 2-8, B lanes 1-3, 7-9, 13-15). Five hours after synthesis, P290R predominantly exist in the monomeric form with very low amounts of oligomers (Figure 2-8, B lane 11). Bands representing the mutant protein are sensitive to both glycosidases (Figure 2-8, B lanes 4-6, 10-12, 16-18). This suggests that although the mutant EAAT1 is N-glycosylated, the sugar residues do not mature. Furthermore, the radiolabeled wildtype protein persists for at least two days post-synthesis indicated a low turnover of the protein in transiently transfected COS7 cells (Figure 2-8, A lane 5,7). In contrast, the mutant protein begins to undergo rapid degradation within hours of being synthesized (Figure 2-8, A lanes 6, 8 B lanes 11, 17).

Thus, the lower abundance of EAAT1-P290R previously reported is not due to decreased protein synthesis but rapid degradation of the mutant protein. The absence of detectable maturely glycosylated mutant protein suggests that the bulk of these immature glycopeptides do not reach the medial Gogli and may be degraded in the ER and early Golgi pathway. This accelerated degradation may be due to defects in protein folding and stability.

In expression studies, co-expressing increasing amounts of P290R while keeping the amount of wildtype construct constant resulted in a dose-dependent decrease in glutamate uptake activity [53]. It is likely that the dominant negative effect observed results from the co-assembly of one or two P290R promoters with wildtype EAAT1. Indeed, pulse-chase analysis demonstrated that P290R, although synthesized at normal levels, undergoes accelerated degradation. In these experiments, I did not observe mature N-glycosylated mutant protein. Confocal microsopy of immunolabeled cells showed that at least some P290R is targeted to the plasma membrane *in vitro* [53]. It is possible that there are low levels of mature P290R present which are not detectable in the pulse-chase gels. Conradt et al reported that although proper glycosylation may be necessary for oligomerization of GLAST, the loss of glycan residues does not alter the function of the transporter *in vitro*[72]. Another explanation would be that some immature mutant protein escapes the Endoplasmic-reticulum-associated protein degradation pathway and are degraded by a downstream surveillance mechanism [73]. Combining pulse-chase with cell surface biotinylation may provide insight.

In summary, I performed experiments to investigate the functional consequences of two additional mutations found in EAAT1: C186S in a family with episodic ataxia and T387P in a family with hemiplegia and migraine and to further understand the molecular mechanism of low protein expression for P290R, found a child with episodic ataxia type 6.

Several lines of evidence suggest that these variants may be pathogenic. *In silico* analysis by several algorithms of phylogenetic conservation and/or functional effect predicted all variants to be damaging (Table 2-1). Moreover, neither of the variants have been reported in the public databases (Table 2-2). I presented empirical data on the effects of the mutations leading to impaired transport of glutamate across the cell membrane *in vitro*.

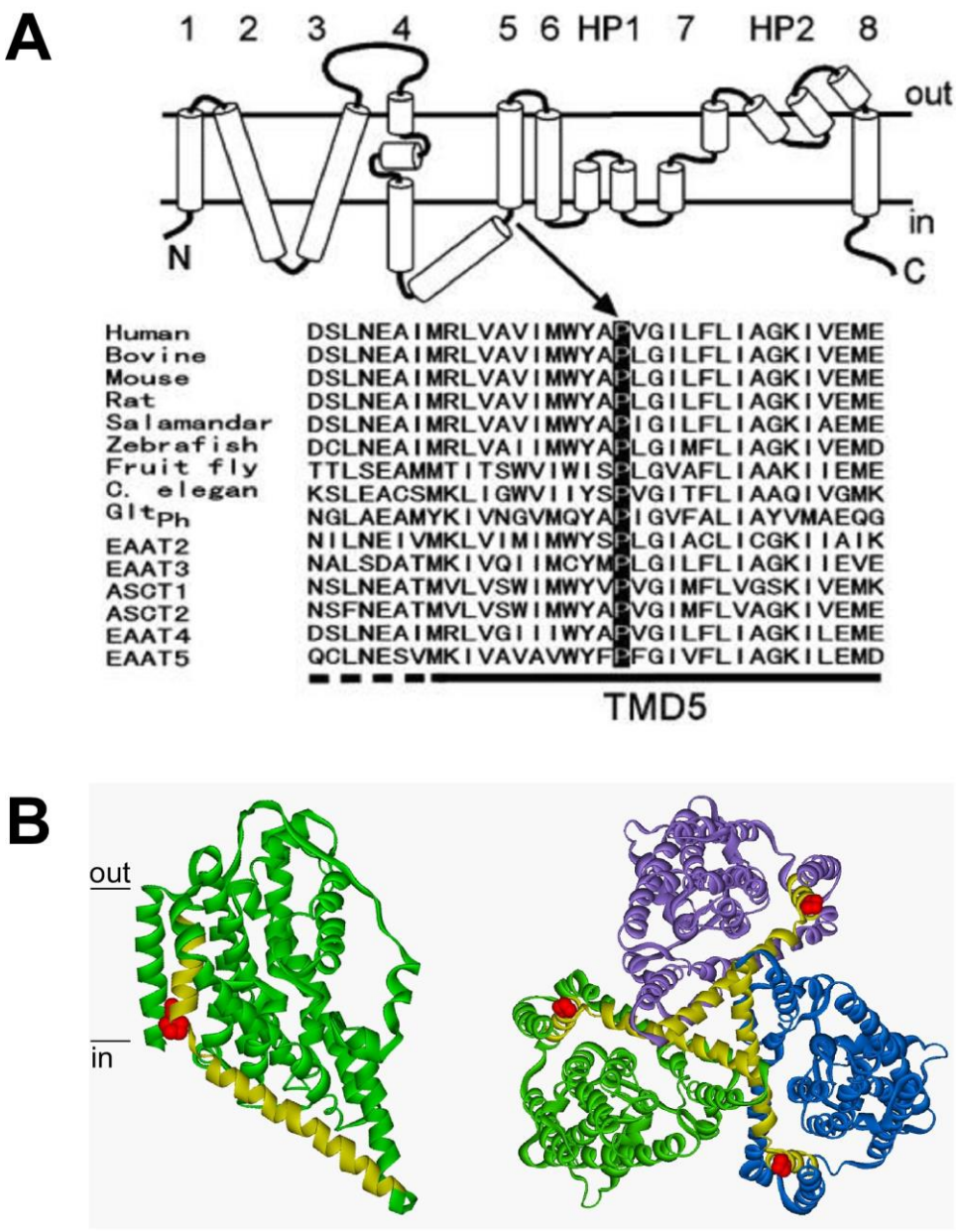

Figure 2-1: The location of P290 in EAAT1. (A) Schematic diagram of the predicted topology of EAAT based on the structure of Gltph [64] showing the location and high conservation of P290 in orthologues. (B) Ribbon diagram of a single Gltph (bacterial) transporter. Three of these promoters come together to form the trimer in (C) yellow represents TM5 and P290 is denoted in red in both (B) and (C). Each color represents a transporter. [53]

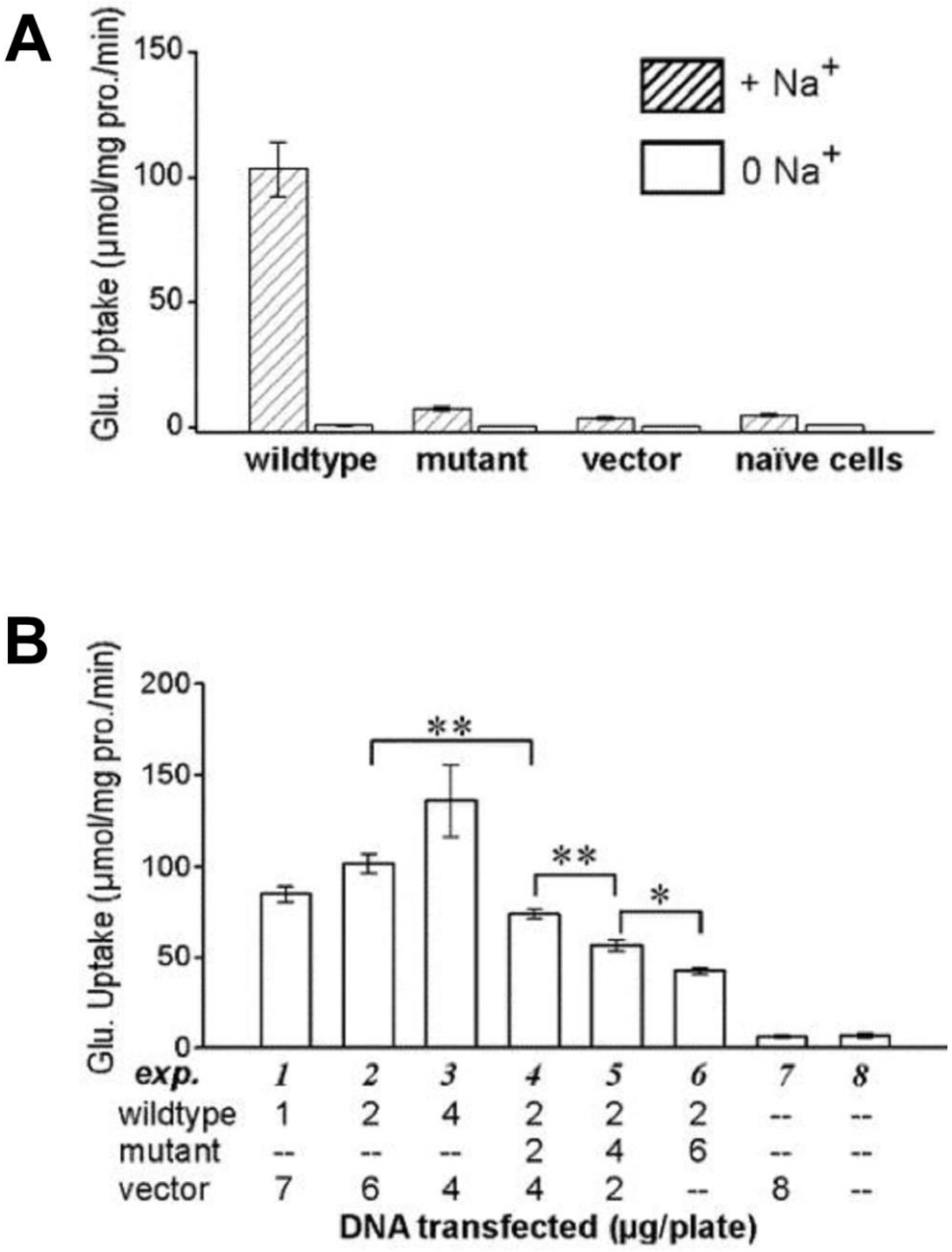

Figure 2-2: Marked reduction in glutamate uptake by P290R. (A) Glutamate uptake in the presence or absence of sodium in cells transiently expressing the indicated construct. Very little sodium dependent glutamate uptake is observed by P290R. (B) Dose dependent decrease of glutamate uptake by cells experssing wildtype EAAT1 with increasing amounts to co-transfected P290R constructs. [53]

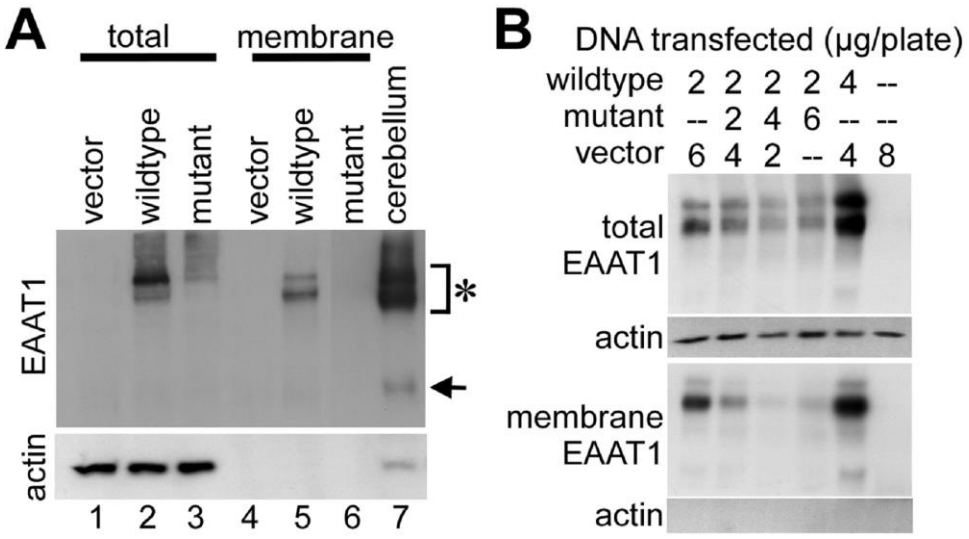

Figure 2-3: Lower expression of P290R EAAT1 by western blot analysis. (A) Biontinylated membrane fractions show decreased expression of P290R at the plasma membrane in transiently transfected cells. Arrow represent monomer, asterisk denotes oligomers (B) Reduced levels of wildtype EAAT1 after coexpression with increasing amounts of mutant P290R construct. [53]

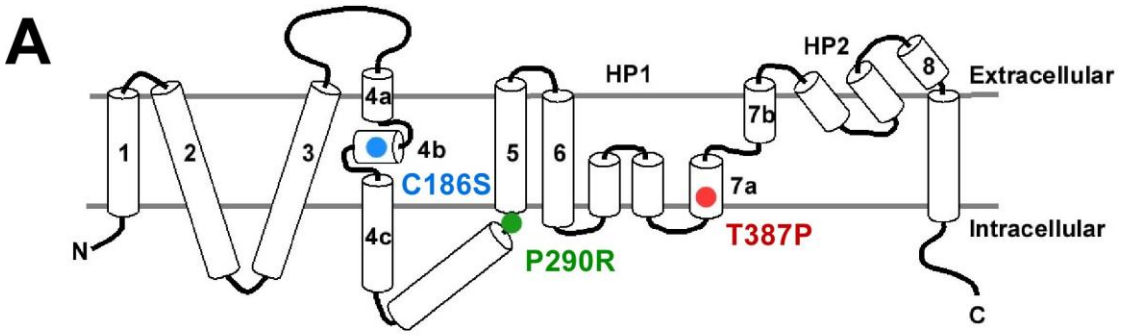

B

Human	PPNLVEACFKQFKTNYE
Bovine	PPNLVEACFKQFKTNYE
Mouse	FPNLVEACFKQFKTSYE
Rat	PPNLVEACFKQFKTSYE
Salamander	PPNMVEACFKQFKTSYE
Zebrafish	PPNLVQACTQQFKTQYG
EAAT2	PENLVQACFQQIQTVTK
EAAT3	PENLVQACFQQYKTK--
EAAT4	PPNLVEACFKQFKTQYS

C

Human	NNGVDKRVTRFVLPVGA
Bovine	NNGVDKRVTRFVLPVGA
Mouse	NNGVDKRITRFVLPVGA
Rat	NNGVDKRITRFVLPVGA
Salamandar	NNKVDKRVTRFVLPVGA
Zebrafish	NNGVDKRVTRFVLPVGA
Fruit fly	NMGIDPRVTRFVIPVGA
C.elegan	NNKVDPRVTRFVLPLGA
EAAT2	NLGIDKRVTRFVLPVGA
EAAT3	NNQVDKRITRFVLPVGA
EAAT4	GLGVDRRITRFVLPVGA

Figure 2-4: Disease causing variants in human EAAT1. (A) Topology of EAAT1 predicted based on the crystal structure of the bacterial homolog Gltph with the locations of the mutations; C186S (blue circle), P290R (green circle), T387P (red circle) (B, C) Conservation of the residues in orthologues and paralogues in other species for C186 in (B) and T387 in (C).

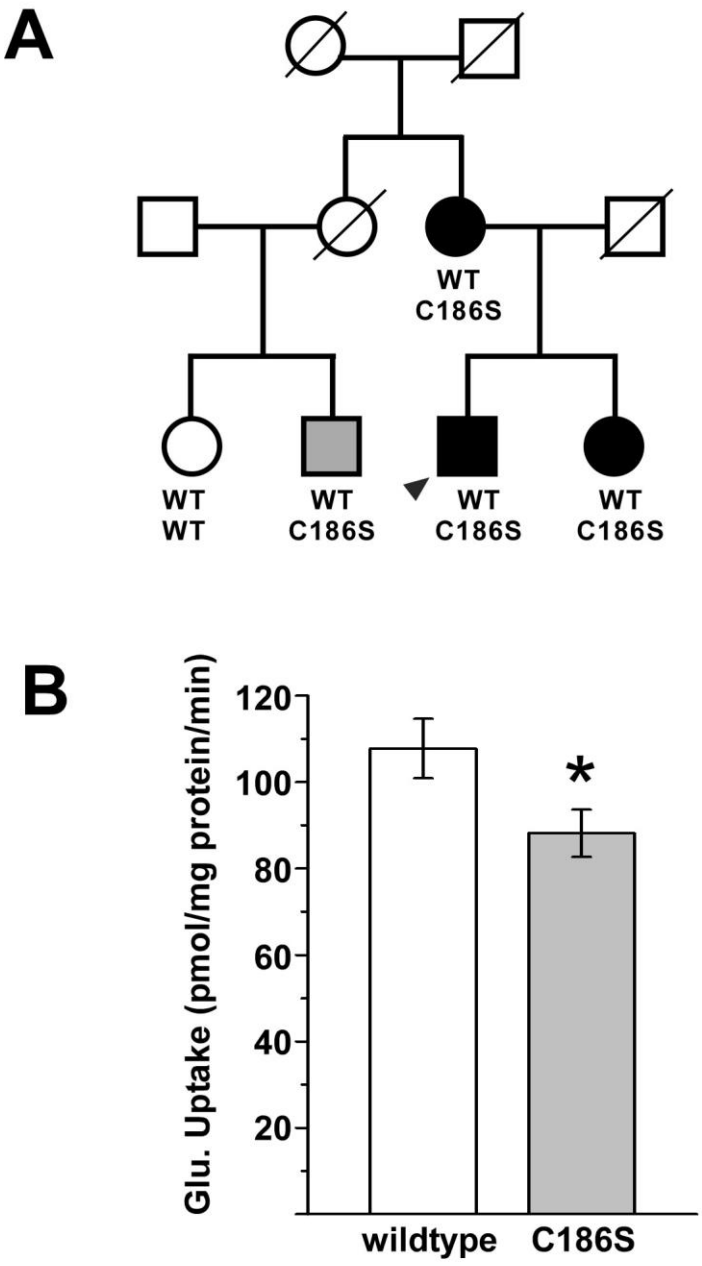

Figure 2-5: Decreased glutamate uptake by EAAT1-C186S mutation. (A) Pedigree of family with heterozygous mutation C186S in EAAT1. Episodic ataxia: filled black circles/squares; Migraine without aura: filled gray square[74]. (B) Modest reduction in glutamate uptake by EAAT1-C186S in COS7 cells transfected with 2ug of plasmid DNA. All values are reported as the mean pmol/mg protein/min glutamate incubation ± SEM for four experiments each done in triplicates; *p=0.029 (student's t-test).

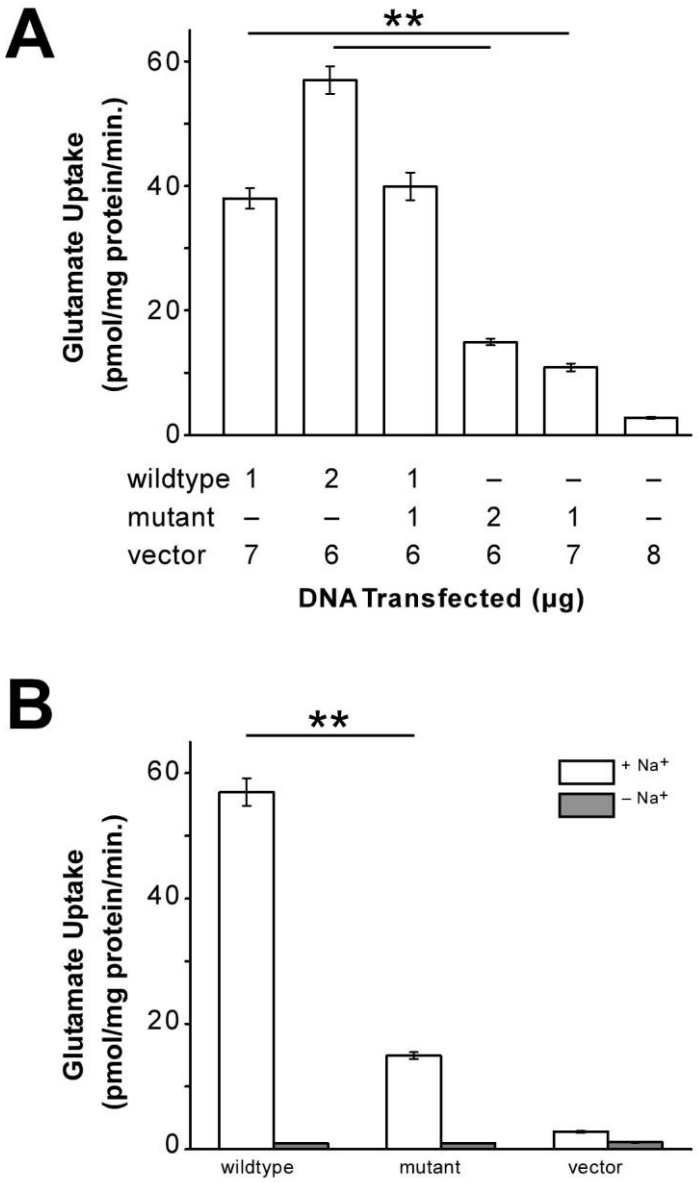

Figure 2-6: Impaired glutamate uptake by EAAT1-T387P. (A) Sodium dependent glutamate uptake assay of wildtype and EAAT1-T387P in COS7 cells transfected with indicated amounts of construct. (B) Glutamate uptake performed in the presence or absence of sodium in COS7 cells transfected with 2ug of wildtype or EAAT1-T387P construct. All values are reported as the mean pmol/mg protein/min glutamate incubation ± SEM for four experiments each done in triplicates; **p<0.001 (student's t-test)

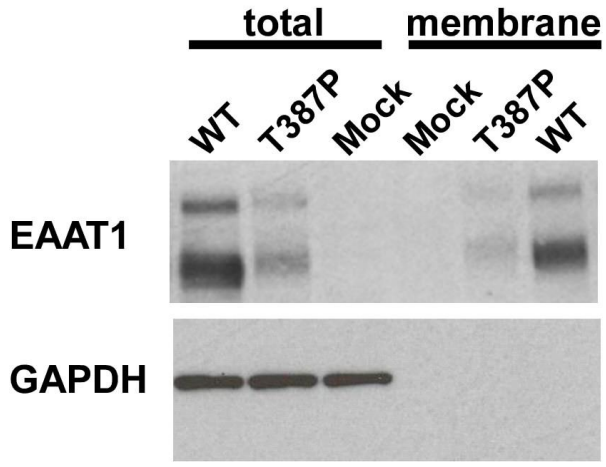

Figure 2-7: Western blot analysis showing decreased abundance of EAAT1-T387P. Transiently transfected cells were labeled with biotin. Total lysate and biotinylated membrane fraction were probed with anti-EAAT1 antibody. GAPDH was probed as a control.

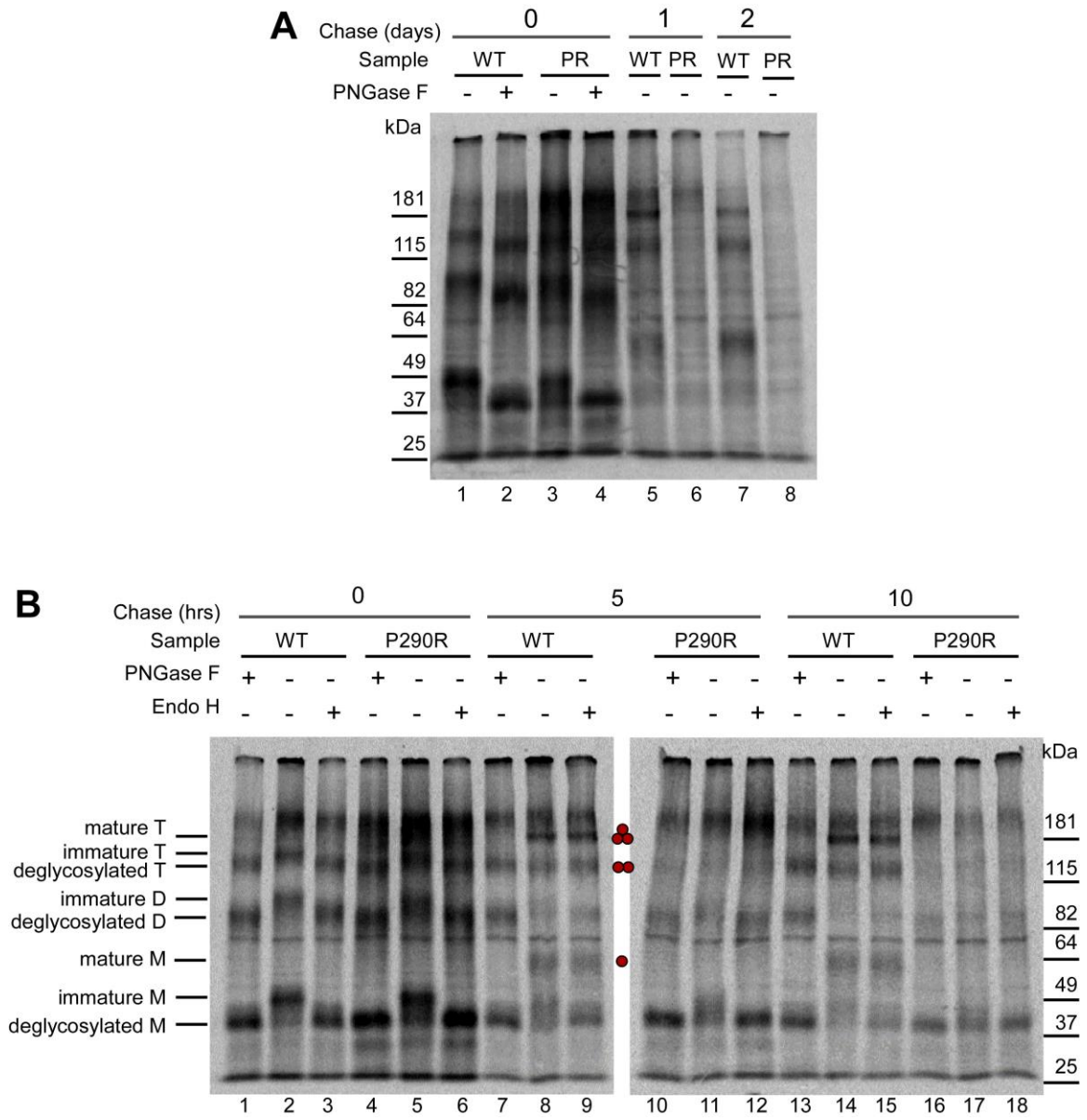

Figure 2-8: EAAT1-P290R undergoes accelerated degradation. Nascent protein was radiolabeled with 35S-Methionine. At the indicated chase time points, EAAT1 was immunoprecipitated, treated with the indicated glycosidase, subject to SDS-PAGE analysis and imaged with a phosphor-imager. (A) Wildtype EAAT1 persists two days after pulse labeling cells. Mutant EAAT1-P290R is synthesized at similar levels to wildtype but is degraded. (B) Wildtype EAAT1 forms mature trimers within 5 hours of labeling cells which is resistant to Endo H digestion. No detectable mature trimers, dimers or monomers are observed for EAAT1-P290R as mutant protein undergoes rapid degradation. Red filled circles indicate mature glycosylated forms of monomer (single circle), dimer (two circles), and trimer (three circles). Monomer (M), Dimer (D), Trimer (T).

Table 2-1. *In Silico* analysis prediction of pathogenicity.

GERP (Genomic Evolutionary Rate Profilling): mendel.stanford.edu/SidowLab/downloads/gerp/Readme.txt Scores greater thatn 3 are predicted to be pathogenic.

PhastCons (Phylogenetic Analysis with Space/Time models): compgen.cshl.edu/phast/phastCons-HOWTO.html Score ranges between 0 and 1 with 1 being highest conservation

Polyphen (Polymorphis Phenotype): http://www.cbs.dtu.dk/services/

SIFT(sorting intolerant from tolerant): sift.jcvi.org

PROVEAN Protein Variation Effect Analyzer: provean.jcvi.org

	C186S	P290R	T387P
phastCons	1	1	1
GERP	5.73	6.07	5.8
PolyPhen	0.838 (possibly damaging)	1 (probably damaging)	0.978 (probably damaging)
SIFT	0.036 (Damaging)	0 (Damaging)	0.001 (Damaging)
PROVEAN	-5.414 (Deleterious)	-8.434 (Deleterious)	-4.386 (Deleterious)

Table 2-2: Frequency of *SLC1A3* mutaitons in the generaly population.

All three EAAT1 mutations have not been reported in large cohorts of samples by exome sequenceing.

The numbers represent the total number of variant observed/total number of alleles tested for the nearest variant.

Exome Aggregation Consortium (ExAC): http://exac.broadinstitute.org/

Database	C186S	P290R	T387P
EXAC variant allele/total allele count	0/121170	0/121410	0/121366
EVS variant allele/total allele count	0/13000	0/13006	0/13006

CHAPTER 3 : *DROSOPHILA MELANOGASTOR* MODEL OF EA6

Introduction

Drosophila express two glial excitatory amino acid transporters (EAAT): EAAT1 and EAAT2 [75, 76]. dEAAT2 primarily transports aspartate with very low affinity for glutamate [77]. dEAAT1 is the only high affinity glial glutamate transporter both in drosophila CNS and the neuromuscular junction (NMJ). Similar to mammalian EAAT1, dEAAT1 uses the gradient of ions to transport glutamate across the plasma membrane and can also function as an anion channel [78]. dEAAT1 is selectively expressed in CNS glia cells in *Drosophila* embryos, larvae and adult [76, 79]. Human and drosophila EAAT1 share 41% homology at the protein level[75]. Knockdown of glial dEAAT1 by RNA interference (RNAi) caused defects in locomotion as they flew poorly and had a poor touch escape response, brain neurophil degeneration, and although can survive as adults, have a reduced lifespan [79]. Utilizing *Drosophila* as an *in vivo* model system to study the pathological mechanism of human mutations in EAAT1 may provide further insight into regulation and impairment of glutamate signaling. To study the effects of P290R-hEAAT1 *in vivo*, I create a fly model expressing a homologous change P243R-EAAT1 in *Drosophila melanogaster*.

Materials and Methods

Cloning and mutagenesis

RNA isolated from the head of Drosophila melanogaster was reverse transcribed with an anchored oligo dT primer and SuperScript First-Strand Synthesis System for RT-PCR (Invitrogen). The full length Drosophila melanogaster EAAT1 (dEAAT1) cDNA was amplified by PCR at a touchdown annealing temperature of 71-64°C using the following primers:

forward primer: 5'-GTTGTCCAGACCCTGAACCAATCCATAG-3'

reverse primer: 5'-GACATGTCCACTCATCGTTTGCGGTTAT-3'

The 1527 bp product was subcloned into pCR-Blunt II TOPO (Invitrogen) with the Zero Blunt TOPO PCR Cloning Kit (Invitrogen). 2 µl of this mixture was transformed into TOP10 competent cells and grown on LB-Kanomycin (50µg/ml) plates. Plasmid DNA was extracted with the QIAprep Spin Miniprep Kit (Qiagen). The P243R mutant construct was generated by site-directed mutagenesis of the wild type cDNA in pCR Blunt II-TOPO using primers dEAAT1-c1114gF and dEAAT1-c1114gR and QuikChange II Site-Directed Mutagenesis Kit according to manufacturer's instructions. All plasmids were bidirectionally sequenced.

For expression studies in Drosophila S2 cell lines, the wild type and mutant dEAAT1 cDNA were cloned into vector pMT/V5-His A (Invitrogen) which contains a Drosophila metallothionein promoter (MT). Expression of the gene is induced upon binding of copper sulfate to the MT promoter. dEAAT1 cDNA in pCR Blunt II-TOPO was excised with EcoR V and Spe I and ligated to compatible ends on pMT/V5-His A digested with EcoR V and Xba I. Ligation was performed with T4 DNA ligase overnight at 16°C. 2 µl of the ligation reaction was transformed into JM109 competent cells (Promega) before plating onto LB-Ampicillin (100µg/ml) plates. Plasmid DNA extracted with the QIAprep Spin Miniprep Kit (Qiagen) or EndoFree Plasmid Maxi Kit (Qiagen). All constructs were validated by bidirectional sequencing.

S2 cell culture and transfection

Drosophila Schneider 2 (S2) cells (Invitrogen) were maintained at room temperature (22-25°C) in Schneider's Drosophila Medium (Invitrogen) supplemented with 10% heat-inactivated fetal bovine serum (FBS; Invitrogen). FBS was heat inactivated at 56°C for 30 min to destroy

complement factors. S2 cells grow as a loosely adherent monolayer which I dissociated by washing the surface of the flask with a pipette. Cells were seeded at a density of $5x10^5$ cells/ml and split before attaining $20x10^6$ cells/ml.

Glutamate Uptake in insect cell lines

Glutamate uptake was measured in Schneider's Drosophila (S2) cells expressing wildtype or P243R mutant dEAAT1 cDNA constructs. dEAAT1-P243R is analogous to the P290R in human EAAT1. $8x10^6$ cells in 5ml culture medium was seeded onto 6 cm tissue culture dishes one day before transient transfection with Fugene 6 (Roche). The next day, 1.5-0.75 µg plasmid DNA was diluted to a final volume of 10 µl with OPTI-MEM reduced serum media (Invitrogen). For each sample, 14µl Fugene 6 was mixed with 176 µl OPTI-MEM and incubated 5 min at room temperature. Once the incubation was complete, this mixture was combined with the diluted plasmid DNA and the reaction incubated for an additional 15 min at room temperature. All 200 µl was applied to cells drop wise and the plate gently rotated to mix. Cells were cultured for five hours, after which the transfection medium was replaced with fresh medium. The following day, expression was induced by treating cells with 500 µM CuSO4 in culture medium. Glutamate uptake was performed 24 hours post induction as described in section chapter II with the following modification: cells were incubated with labeled glutamate uptake buffer for 5 min. Mock transfected cells were transfected with an identical plasmid but lacking the dEAAT1 gene.

Generation of transgenic Fruit flies

Wild type and mutant dEAAT1 cDNA was excised from pCR Blunt II-TOPO with EcoR V and Spe I and ligated to compatible ends on a Stu I and Xba I digested pExPress-UAS plasmid. All constructs were bidirectionally sequenced.

Fruit flies with the transgene UAS-dEAAT1, carrying either the wildtype or mutant P243R dEAAT1 cDNA under the control of the UAS-GAL4 regulatory system were generated by the Duke Model Systems Genomics (Figure 3-1). By crossing these flies with GAL4 driver lines, dEAAT1 will be expressed only in cells which also express GAL4. This binary upstream activating sequence (UAS)-GAL4 system allows for conditional expression of the transgene enabling spatial and temporal gene expression.

Fly maintenance

Flies were grown in standard cornmeal molasses agar media in bottles or vials under a 12 hour light-dark cycle. All crosses were performed at 25°C. Stocks were maintained at 18°C and flipped as needed. Flies were crossed using standard methods.

Survival assay in transgenic fruit flies

Juicy agar plates were prepared by melting 8.75g bacto-agar in 250 ml of ddH2O by autoclave. 250 ml of a filtered sterile juice solution (6.25g sucrose, 125 ml Welch grape juice) was mixed in and poured into 60 cm petri dishes and allowed to solidify. Freshly prepared yeast paste (.25g dry yeast powder, .325 ml ddH2O) was applied to the center of each plate prior to use. Survival assays were performed using standard methods.

Mapping the transgene integration sites in the mutant D.mel

Inverse PCR and sanger sequencing were utilized to map the transgene integration site within the drosophila genome in relevant lines. Genomic DNA was extracted from 10 adult flies. Flies were homogenized in 70 µl lysis buffer using a Knotes disposable tissue grinder. An equal volume of lysis buffer was added and the tissue further grinded until only cuticles remained. Samples were incubated at 65°C for 30 min. Protein and cellular debri were precipitated with 270 µl LiCl/KAc buffer on ice for at least 10 min followed by a 15 min

centrifugation at 12,000 rpm. The clarified supernatant was transferred to a new centrifuge tube and DNA precipitated with 60% (v/v) of isopropanol. After spinning at 12000 rpm for 15 min, the pellet was washed with an equal volume of 70% (v/v) ethanol. This DNA pellet was reconstituted in TE Buffer (10mM Tris, 1mM EDTA pH 8.0) and quantified by NanoDrop.
Lysis Buffer: 100mM Tris-Cl, 100mM EDTA, 100mM NaCl, 0.5% SDS (w/v) pH 7.5
LiCl/KAc Buffer: 1.4M potassium acetate, 4.3M lithium chloride (store at 4°C)

1-2 µg of genomic DNA was digested with 20 units of HinP1 I (New England BioLabs) in the presence of 0.2µg RNase A in 25µl at 37°C for 3hours to overnight. 5 µl equivalent were analyzed on 0.8% agarose gel to confirm that the digest was successful (no high molecular weight bands and presence of low molecular weight shmearing on the gel) before inactivating the enzyme at 65°C for 20 min. This mixture was ligated overnight at 4°C in a large volume which dilutes the DNA and favors self-ligation. DNA was precipitated with 40µl of 3M sodium acetate and 1 ml ethanol. After a 20 min incubation at -20°C, samples were spun at 12000rpm for 10 min. The pellet was washed with 70% (v/v) ethanol, air-dried to remove residual ethanol, and reconstituted with TE buffer pH8.0. 2-5µl of the purified ligation product was PCR amplified using primer sets flanking the 5' and 3' ends of the transgene. Amplicons were cleaned-up or treated with enzymes ExoI/SAP (section) then sanger sequenced. Reads were mapped to both the UCSC genome browser and Flybae to ascertain the genomic sequence flanking the transgene. w1118(CS)10 was used as a negative control.

Results

Insect cell lines expressing dEAAT1-P243R demonstrated markedly impaired glutamate transport

To test whether the fruit fly would be a good animal model for EA6, it was important to first test if the homologous mutation in *Drosophila* EAAT1 (dEAAT1) would alter glutamate uptake *in vitro.* There was a profound loss of glutamate uptake by cells expressing mutant dEAAT1 (0.93 ± 0.19) compared to wildtype (10.84 ± 0.9) (Figure 3-2). Furthermore, co-expression of equal molar ratios of wildtype and P243R-dEAAT1 constructs showed that mutant transporter interfered with the wildtype function: 3.38 ± 0.17 (0.75 ugWT+0.75 ug P243R) versus 10.84 ± 0.9 (0.75 ug WT only) (Figure 3-2). All values are reported as the mean pmol/mg protein/min glutamate incubation ± standard error of the mean (SEM). The remarkable similarity of effects on glutamate uptake activity between heterologous expression studies in mammalian cells and its *Drosophila* homologue in insect cell lines (taken together with the published dEAAT1 RNAi models) suggested that *Drosophila* may be a good model system to understand how glutamate transporter dysfunction may lead to neurological symptoms in EA6.

Transgenic flies expressing P243R-dEAAT1 had reduced life span

Several isolated lines were identified based on eye color and chromosomal integration sites. Of these 8-10 lines each for wildtype or mutant were crossed with various GAL4 driver lines for conditional expression of the dEAAT1 transgene either ubiquitously or in specific cells. Of these WB16B carrying the wildtype transgene and PRC6A harboring the P243R mutant transgene were chosen for further characterization. Regardless of which driver was used, embryos expressing the wildtype transgene developed into adult flies (Figure 3-3). Embryos

which expressed mutant EAAT1 ubiquitously (Daughterless-GAL4) in all cells never developed into larvae (Figure 3-3). In contrast, most embryos expressing the mutant transgene specifically in glial cells (REPO-GAL4, dEAAT1-GAL4) developed into larvae but progressively died with no or few viable adults (Figure 3-3). Remarkably, when the mutant transgene was expressed only in neurons (Elav-GAL4, dVGluT-GAL4) embryos had a normal life span comparable to those expressing the wildtype transgene (Figure 3-3).

Wildtype line WB16B bears the wildtype transgene on left arm of chromosome 3 with the 5' mapping to 639590 and the 3' mapping to 639583 in the reverse direction. It does not disrupt any known transcripts. The mutant transgene in line PRC6A, located on the right arm of chromosome 3, is flanked by 1090646 on the 5' and 1090639 on the 3' end. Although, it integrated into a intron in the Hph gene, fruit flies not expressing the transgene do not show any defects in development, growth, or survival.

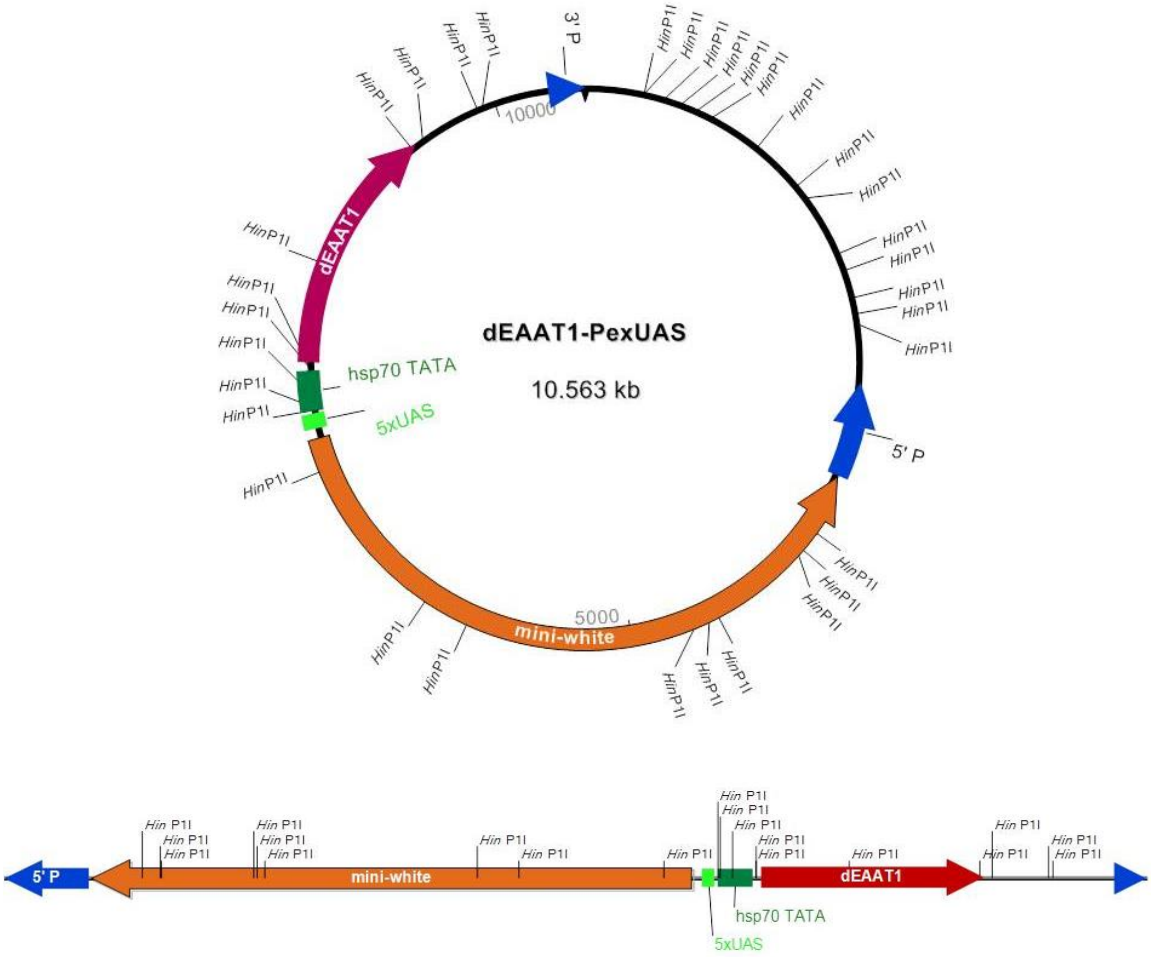

Figure 3-1: dEAAT1-PEX-UAS construct used to generate transgenic Fruit flies. (A) Circularized plasmid with labeled transgene and regulatory elements (B) The portion in the plasmid in (A) which integrates into the fly genome mediated by the flanking 5' and 3' P elements (blue arrow/arrowhead). dEAAT1: WT or P243R glutamate transporter transgene, mini-white gene to identify transgenic fruit flies, 5xUAS (Upstream activated sequence) for conditional transgene expression.

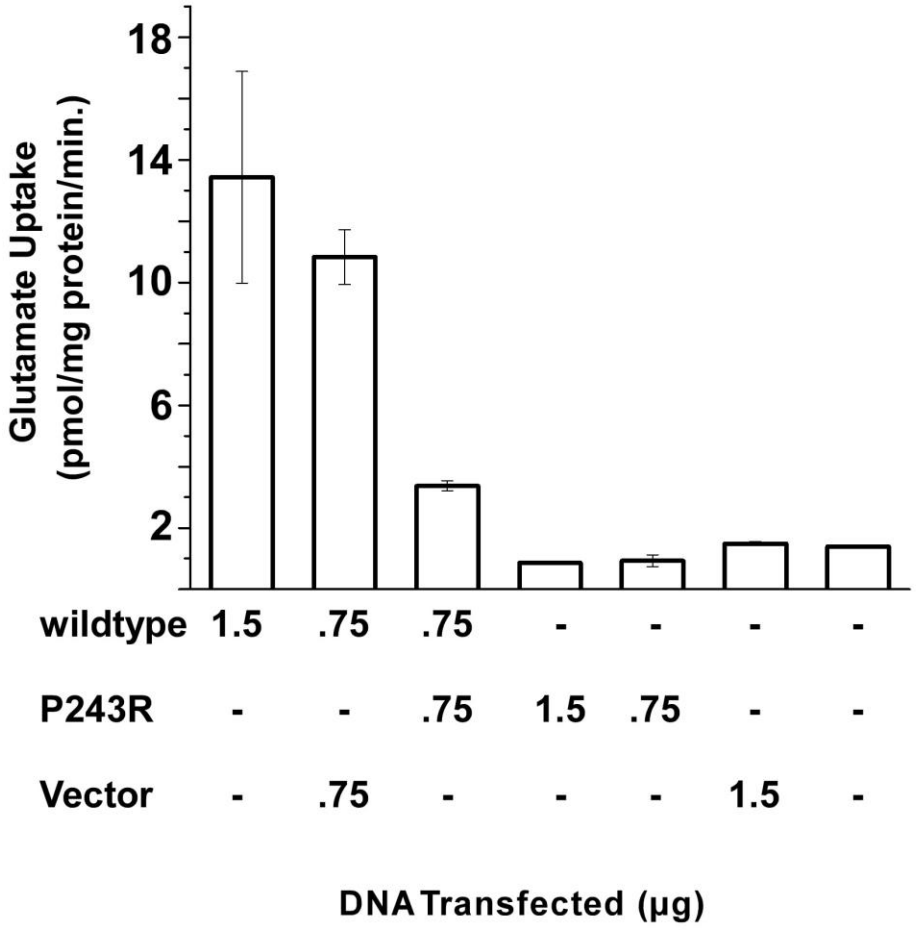

Figure 3-2: Markedly reduced glutamate uptake by dEAAT1-P243R. Sodium dependent glutamate uptake assay of wildtype and dEAAT1-P243R in S2 insect cell lines transfected with indicated amounts of construct shows dramatically reduced uptake by mutant protein. Co-expression of the mutant also disrupted glutamate uptake by wildtype dEAAT1. All values are reported as the mean pmol/mg protein/min glutamate incubation ± SEM

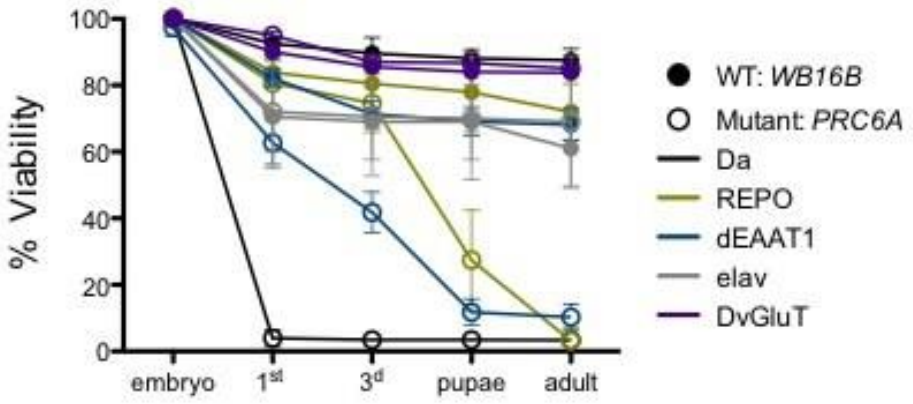

Figure 3-3: Survival assay showing P243R-dEAAT1 transgenic flies have shortened lifespan with ubiquitous or glial specific transgene expression. UAS-WT or UAS-P243R (homologous to P290R mutation that causes EA6) were crossed to the following driver GAL4 lines: Da (Daughterless for ubiquitous expression), REPO (for expression in glia), dEAAT1 (to express transgene specifically in cells that produce endogenous glutamate transporter), elav (to express in neurons) and dVGluT (to drive transgene expression in subset of neurons which express the vesicular glutamate transporter). WT (filled circles), P243R (open circles).

CHAPTER 4 : DISCUSSION AND CONCLUSION

Is there genotype-phenotype correlation? Does glutamate uptake impairment correlate with the clinical manifestations?

The data that I presented in Chapter 2 showed that C186S and T387P led to diminished glutamate uptake *in vitro*, which suggest that the respective genetic variants may be pathogenic. The survival data from Chapter 3 suggest that the transgenic fruit flies may be a valid model for EA6, since the mutant fruit flies demonstrated robust phenotypes, with the most severe phenotype found in those that express the mutant protein in glia, which best recapitulates the condition in patients. Furthermore, clinical severity appears to correlate with *in vitro* disruption of glutamate transport activity in that the severity Case 1> Case 3 > Case 2 was correlated with the same degree of impairment in transporter function P290R> T378P> C186S.

P290R resulted in near complete loss of glutamate uptake (93% reduction) *in vitro* and is associated with the most severe symptoms (more severe attacks of episodic ataxia, alternating hemiplegia, seizures, progressive ataxia and migraine) [53]. This mutation also had a dominant negative effect on glutamate uptake by the wildtype transporter and protein stability of wildtype EAAT1 [53]. T378P associated with hemiplegic migraine results in a substantive 75% reduction in glutamate uptake. The associated phenotype is mild in caparison to P290R, albeit with overlapping symptoms of hemiplegia and migraine. In contrast, C186S which results in a modest 18% decrease in glutamate uptake is associated with episodic ataxia. Thus, although the three different mutations in EA6 result in distinct clinical manifestations, there are shared symptoms.

Since only three disease-causing mutations have been functionally investigated, it is impossible to make definitive statements regarding correlations, and additional confirmation is required. Advancements in genetic technology and precision medicine would allow more individuals to gain access to exome or whole genome sequencing, facilitating the identification of increasing number of mutations in *SLC1A3*.

How else could the mutations alter transporter function to cause symptoms?

In my thesis work, I performed biochemical studies on the mutant and the wildtype transporters to show that diminished mutant proteins (due to accelerated degradation in the case of P290R) contributed to the overall impaired glutamate uptake. I did not examine changes in the biophysical properties of the mutant transporters, which should be further investigated to better define the structure-function correlation.

Indeed, how the glutamate transporter couples sodium, potassium, and anions to move glutamate across the cell membrane remains incompletely understood. The mutations linked to human disease provide important clues to help clarify and define functional domains within the glutamate transporter. Using electrophysiology, Winter et al showed that P290R increases the anion current by EAAT1, independent of substrate levels *in vitro* [80]. They proposed that P290R causes the channel to stay in an open state.

Additional confirmation comes from a report published by the Amara group, which elegantly shows that substitution of an Arginine 388 in EAAT1 to negatively charged acidic residues Aspartic or Glutamic acid alters channel gaiting and causes the channel to remain in an open state [69]. The increased anion currents were not affected by sodium concentration[69]. They hypothesize that this residue may be crucial for gating the substrate-gated anion

conductance [69]. Interestingly, this residue is adjacent to Threonine 387. Like T387P, both R388D and R388E showed drastically reduces cell surface expression and glutamate uptake by R388D and R388E[69]. In a separate report mutation of nearby residues K384 and R385 lead to increased anion currents [81].

What does the Drosophila model suggest?

In Chapter 3, through creating a fruit fly model for EA6, I show that driving the expression of the transgene in glia resulted in reduced survival of flies harboring mutant not wildtype transgene, with few mutant flies developing into adults. When the wildtype or mutant transgene were expressed in neurons, both wildtype and mutant flies developed normally. RNAi meditated knockdown of glial dEAAT1 showed that although the flies had shortened lifespan, they were able to grow into adults [79]. Subsequent work published by Stacey et al showed that dEAAT1 null flies had locomotion defects that could be rescued by expressing dEAAT1 in a subset of glia near glutamatergic synapsis [82]. That expression of P243R-dEAAT1 transgene is more toxic to flies than the knockout, suggests that P243R-dEAAT1 has a toxic effect on glial. A recent report describes transgenic fruit fly larvae harboring the identical mutation, P243R-dEAAT1 [83]. Expression of the mutant transgene in glia resulted in motility defects, transient paralysis and decreased astrocyte infiltration. They hypothesized that the effects may be due to abnormal anion conductance. Co-expression of Ncc69, a sodium potassium chloride co-transporter which drives anion uptake into cells, rescued the phenotype in flies expressing the mutant transgene in glia.

What is the phenotypic spectrum of EA6? How do mutations lead to disease?

The challenge in defining the clinical spectrum of EA6 is the rarity of the syndrome. The clearest genotype-phenotype data we have are on Case 1, who has a unique mutation with a unique phenotype with episodic ataxia and progressive ataxia with cerebellar atrophy, epilepsy, and hemiplegic migraine. Case 2 has episodic ataxia but the genotype C186S is also found in relatives with migraine without episodic ataxia. Case 3 has hemiplegic migraine who inherited T387P from his father with migraine without aura. Based on the findings from these three cases, there appear to be overlapping features spanning episodic ataxia and migraine of variable severity.

Findings from mouse models of FHM1 suggest that FHM1 mutations lead to cortical hyperexcitability and [84] enhanced susceptibility to spreading depression [85] hypothesized to be due to increased glutamate release. It is therefore an attractive hypothesis that impaired glial glutamate reuptake may be functionally similar to increased glutamate release. It is my hope that further studies on the transgenic fruit flies may help us understand how mutant glial glutamate transporters may cause early death and that new drugs may be discovered to rescue the phenotype.

REFERENCES

1. OMIM,
Online Mendelian Inheritance in Man, OMIM.

2. Litt, M., et al., *Episodic Ataxia Myokymia Syndrome Is Associated with Point Mutations in the Human Potassium Channel Gene Kcna1 (Kv1.1).* Journal of General Physiology, 1994. **104**(6): p. A10-A10.

3. Graves, T.D., et al., *Episodic ataxia type 1: clinical characterization, quality of life and genotype-phenotype correlation.* Brain, 2014. **137**: p. 1009-1018.

4. Zuberi, S.M., et al., *A novel mutation in the human voltage-gated potassium channel gene (Kv1.1) associates with episodic ataxia type 1 and sometimes with partial epilepsy.* Brain, 1999. **122 (Pt 5)**: p. 817-25.

5. D'Adamo, M.C., et al., *New insights into the pathogenesis and therapeutics of episodic ataxia type 1.* Frontiers in Cellular Neuroscience, 2015. **9**.

6. Litt, M., et al., *A Gene for Episodic Ataxia/Myokymia Maps to Chromosome 12p13.* American Journal of Human Genetics, 1994. **55**(4): p. 702-709.

7. Browne, D.L., et al., *Episodic Ataxia Myokymia Syndrome Is Associated with Point Mutations in the Human Potassium Channel Gene, Kcna1.* Nature Genetics, 1994. **8**(2): p. 136-140.

8. Olesen, J. and T.J. Steiner, *The international classification of headache disorders, 2nd edn (ICDH-II).* Journal of Neurology Neurosurgery and Psychiatry, 2004. **75**(6): p. 808-811.

9. Baloh, R.W., et al., *Familial episodic ataxia: clinical heterogeneity in four families linked to chromosome 19p.* Ann Neurol, 1997. **41**(1): p. 8-16.

10. Jen, J., G.W. Kim, and R.W. Baloh, *Clinical spectrum of episodic ataxia type 2.* Neurology, 2004. **62**(1): p. 17-22.

11. Imbrici, P., et al., *Late-onset episodic ataxia type 2 due to an in-frame insertion in CACNA1A.* Neurology, 2005. **65**(6): p. 944-6.

12. Mori, Y., et al., *Primary structure and functional expression from complementary DNA of a brain calcium channel.* Nature, 1991. **350**(6317): p. 398-402.

13. Ophoff, R.A., et al., *Familial hemiplegic migraine and episodic ataxia type-2 are caused by mutations in the Ca2+ channel gene CACNL1A4.* Cell, 1996. **87**(3): p. 543-552.

14. Zhuchenko, O., et al., *Autosomal dominant cerebellar ataxia (SCA6) associated with small polyglutamine expansions in the alpha 1A-voltage-dependent calcium channel.* Nat Genet, 1997. **15**(1): p. 62-9.

15. Denier, C., et al., *High prevalence of CACNA1A truncations and broader clinical spectrum in episodic ataxia type 2.* Neurology, 1999. **52**(9): p. 1816-21.

16. Wan, J., et al., *CACNA1A mutations causing episodic and progressive ataxia alter channel trafficking and kinetics.* Neurology, 2005. **64**(12): p. 2090-7.

17. Wan, J., et al., *Large Genomic Deletions in CACNA1A Cause Episodic Ataxia Type 2.* Front Neurol, 2011. **2**: p. 51.

18. Labrum, R.W., et al., *Large scale calcium channel gene rearrangements in episodic ataxia and hemiplegic migraine: implications for diagnostic testing.* J Med Genet, 2009. **46**(11): p. 786-91.

19. Steckley, J.L., et al., *An autosomal dominant disorder with episodic ataxia, vertigo, and tinnitus.* Neurology, 2001. **57**(8): p. 1499-502.

20. Cader, M.Z., et al., *A genome-wide screen and linkage mapping for a large pedigree with episodic ataxia.* Neurology, 2005. **65**(1): p. 156-8.

21. Farmer, T.W. and V.M. Mustian, *Vestibulocerebellar ataxia. A newly defined hereditary syndrome with periodic manifestations.* Arch Neurol, 1963. **8**: p. 471-80.

22. Damji, K.F., et al., *Periodic vestibulocerebellar ataxia, an autosomal dominant ataxia with defective smooth pursuit, is genetically distinct from other autosomal dominant ataxias.* Arch Neurol, 1996. **53**(4): p. 338-44.

23. ExAC, *Exome Aggregation Consortium*

24. Kerber, K.A., et al., *A new episodic ataxia syndrome with linkage to chromosome 19q13.* Arch Neurol, 2007. **64**(5): p. 749-52.

25. Conroy, J., et al., *A novel locus for episodic ataxia:UBR4 the likely candidate.* Eur J Hum Genet, 2014. **22**(4): p. 505-10.

26. Kramer, P.L., et al., *A Locus for the Nystagmus-Associated Form of Episodic Ataxia Maps to an Ii-Cm Region on Chromosome 19p.* American Journal of Human Genetics, 1995. **57**(1): p. 182-185.

27. Teh, B.T., et al., *Familial Periodic Cerebellar-Ataxia without Myokymia Maps to a 19-Cm Region on 19p13.* American Journal of Human Genetics, 1995. **56**(6): p. 1443-1449.

28. Vonbrederlow, B., et al., *Mapping the Gene for Acetazolamide Responsive Hereditary Paryoxysmal Cerebellar-Ataxia to Chromosome 19p.* Human Molecular Genetics, 1995. **4**(2): p. 279-284.

29. Russell, M.B. and A. Ducros, *Sporadic and familial hemiplegic migraine: pathophysiological mechanisms, clinical characteristics, diagnosis, and management.* Lancet Neurology, 2011. **10**(5): p. 457-470.

30. Thomsen, L.L., et al., *A population-based study of familial hemiplegic migraine suggests revised diagnostic criteria.* Brain, 2002. **125**: p. 1379-1391.

31. Jurkat-Rott, K., et al., *Variability of familial hemiplegic migraine with novel A1A2 Na+/K+-ATPase variants.* Neurology, 2004. **62**(10): p. 1857-1861.

32. Ducros, A., et al., *The clinical spectrum of familial hemiplegic migraine associated with mutations in a neuronal calcium channel.* New England Journal of Medicine, 2001. **345**(1): p. 17-U5.

33. Vahedi, K., et al., *CACNA1A gene de novo mutation causing hemiplegic migraine, coma, and cerebellar atrophy.* Neurology, 2000. **55**(7): p. 1040-1042.

34. Hansen, J.M., et al., *Trigger factors for familial hemiplegic migraine.* Cephalalgia, 2011. **31**(12): p. 1274-1281.

35. Jen, J., et al., *A novel nonsense mutation in CACNA1A causes episodic ataxia and hemiplegia.* Neurology, 1999. **53**(1): p. 34-37.

36. De Fusco, M., et al., *Haploinsufficiency of ATP1A2 encoding the Na+/K+ pump alpha 2 subunit associated with familial hemiplegic migraine type 2.* Nature Genetics, 2003. **33**(2): p. 192-196.

37. Spadaro, M., et al., *A G301R Na(+)/K(+)-ATPase mutation causes familial hemiplegic migraine type 2 with cerebellar signs.* Neurogenetics, 2004. **5**(3): p. 177-185.

38. Fernandez, D.M., et al., *A novel ATP1A2 gene mutation in an irish familial hemiplegic migraine kindred.* Headache, 2008. **48**(1): p. 101-108.

39. Dichgans, M., et al., *Mutation in the neuronal voltage-gated sodium channel SCN1A in familial hemiplegic migraine.* Lancet, 2005. **366**(9483): p. 371-377.

40. Fan, C., et al., *Early-onset familial hemiplegic migraine due to a novel SCN1A mutation.* Cephalalgia, 2016.

41. Vanmolkot, K.R.J., et al., *The novel L1649Q mutation in the SCN1A epilepsy gene is associated with familial hemiplegic migraine: genetic and functional studies.* Cephalalgia, 2006. **26**(11): p. 1365-1366.

42. Weller, C.M., et al., *Two novel SCNIA mutations identified in families with familial hemiplegic migraine.* Cephalalgia, 2014. **34**(13): p. 1062-1069.

43. Cestele, S., et al., *Divergent effects of the T1174S SCN1A mutation associated with seizures and hemiplegic migraine.* Epilepsia, 2013. **54**(5): p. 927-935.

44. Castro, M.J., et al., *First mutation in the voltage-gated Na(V)1.1 subunit gene SCN1A with co-occurring familial hemiplegic migraine and epilepsy.* Cephalalgia, 2009. **29**(3): p. 308-313.

45. Vahedi, K., et al., *Elicited repetitive daily blindness A new phenotype associated with hemiplegic migraine and SCN1A mutations.* Neurology, 2009. **72**(13): p. 1178-1183.

46. Sweney, M.T., et al., *Alternating Hemiplegia of Childhood: Early Characteristics and Evolution of a Neurodevelopmental Syndrome.* Pediatrics, 2009. **123**(3): p. e534-e541.

47. Panagiotakaki, E., et al., *Evidence of a non-progressive course of alternating hemiplegia of childhood: study of a large cohort of children and adults.* Brain, 2010. **133**: p. 3598-3610.

48. Bassi, M.T., et al., *A novel mutation in the ATP1A2 gene causes alternating hemiplegia of childhood.* Journal of Medical Genetics, 2004. **41**(8): p. 621-628.

49. Swoboda, K.J., et al., *Alternating hemiplegia of childhood or familial hemiplegic migraine?: A novel ATP1A2 mutation.* Annals of Neurology, 2004. **55**(6): p. 884-887.

50. Heinzen, E.L., et al., *De novo mutations in ATP1A3 cause alternating hemiplegia of childhood.* Nature Genetics, 2012. **44**(9): p. 1030-+.

51. Panagiotakaki, E., et al., *Clinical profile of patients with ATP1A3 mutations in Alternating Hemiplegia of Childhood-a study of 155 patients.* Orphanet Journal of Rare Diseases, 2015. **10**.

52. de Vries, B., et al., *CACNA1A mutation linking hemiplegic migraine and alternating hemiplegia of childhood.* Cephalalgia, 2008. **28**(8): p. 887-891.

53. Jen, J.C., et al., *Mutation in the glutamate transporter EAAT1 causes episodic ataxia, hemiplegia, and seizures.* Neurology, 2005. **65**(4): p. 529-34.

54. Freilinger, T., et al, *A novel mutation in SLC1A3 associated with pure hemiplegic migraine.* JOURNAL OF HEADACHE AND PAIN., 2010. **11**.

55. Fonnum, F., *Glutamate - a Neurotransmitter in Mammalian Brain.* Journal of Neurochemistry, 1984. **42**(1): p. 1-11.

56. Danbolt, N.C., *Glutamate uptake.* Progress in Neurobiology, 2001. **65**(1): p. 1-105.

57. Vandenberg, R.J. and R.M. Ryan, *Mechanisms of Glutamate Transport.* Physiological Reviews, 2013. **93**(4): p. 1621-1657.

58. Arriza, J.L., et al., *Excitatory amino acid transporter 5, a retinal glutamate transporter coupled to a chloride conductance.* Proc Natl Acad Sci U S A, 1997. **94**(8): p. 4155-60.

59. Arriza, J.L., et al., *Functional comparisons of three glutamate transporter subtypes cloned from human motor cortex.* J Neurosci, 1994. **14**(9): p. 5559-69.

60. Fairman, W.A., et al., *An excitatory amino-acid transporter with properties of a ligand-gated chloride channel.* Nature, 1995. **375**(6532): p. 599-603.

61. Banner, S.J., et al., *The expression of the glutamate re-uptake transporter excitatory amino acid transporter 1 (EAAT1) in the normal human CNS and in motor neurone disease: an immunohistochemical study.* Neuroscience, 2002. **109**(1): p. 27-44.

62. Chaudhry, F.A., et al., *Glutamate transporters in glial plasma membranes: highly differentiated localizations revealed by quantitative ultrastructural immunocytochemistry.* Neuron, 1995. **15**(3): p. 711-20.

63. Lehre, K.P. and N.C. Danbolt, *The number of glutamate transporter subtype molecules at glutamatergic synapses: chemical and stereological quantification in young adult rat brain.* J Neurosci, 1998. **18**(21): p. 8751-7.

64. Yernool, D., et al., *Structure of a glutamate transporter homologue from Pyrococcus horikoshii.* Nature, 2004. **431**(7010): p. 811-818.

65. Boudker, O., et al., *Coupling substrate and ion binding to extracellular gate of a sodium-dependent aspartate transporter.* Nature, 2007. **445**(7126): p. 387-93.

66. Reyes, N., C. Ginter, and O. Boudker, *Transport mechanism of a bacterial homologue of glutamate transporters.* Nature, 2009. **462**(7275): p. 880-5.

67. Haugeto, O., et al., *Brain glutamate transporter proteins form homomultimers.* J Biol Chem, 1996. **271**(44): p. 27715-22.

68. Yernool, D., et al., *Trimeric subunit stoichiometry of the glutamate transporters from Bacillus caldotenax and Bacillus stearothermophilus.* Biochemistry, 2003. **42**(44): p. 12981-12988.

69. Torres-Salazar, D., et al., *A Mutation in Transmembrane Domain 7 (TM7) of Excitatory Amino Acid Transporters Disrupts the Substrate-dependent Gating of the Intrinsic Anion Conductance and Drives the Channel into a Constitutively Open State.* Journal of Biological Chemistry, 2015. **290**(38): p. 22977-22990.

70. Koch, H.P., J.M. Hubbard, and H.P. Larsson, *Voltage-independent sodium-binding events reported by the 4B-4C loop in the human glutamate transporter excitatory amino acid transporter 3.* Journal of Biological Chemistry, 2007. **282**(34): p. 24547-24553.

71. Huang, S.W. and R.J. Vandenberg, *Mutations in transmembrane domains 5 and 7 of the human excitatory amino acid transporter 1 affect the substrate-activated anion channel.* Biochemistry, 2007. **46**(34): p. 9685-9692.

72. Conradt, M., T. Storck, and W. Stoffel, *Localization of N-Glycosylation Sites and Functional-Role of the Carbohydrate Units of Glast-1, a Cloned Rat-Brain L-Glutamate L-Aspartate Transporter.* European Journal of Biochemistry, 1995. **229**(3): p. 682-687.

73. Ellgaard, L., M. Molinari, and A. Helenius, *Setting the standards: quality control in the secretory pathway.* Science, 1999. **286**(5446): p. 1882-8.

74. de Vries, B., et al., *Episodic ataxia associated with EAAT1 mutation C186S affecting glutamate reuptake.* Arch Neurol, 2009. **66**(1): p. 97-101.

75. Besson, M.T., L. Soustelle, and S. Birman, *Identification and structural characterization of two genes encoding glutamate transporter homologues differently expressed in the nervous system of Drosophila melanogaster.* FEBS Lett, 1999. **443**(2): p. 97-104.

76. Soustelle, L., et al., *Terminal glial differentiation involves regulated expression of the excitatory amino acid transporters in the Drosophila embryonic CNS.* Dev Biol, 2002. **248**(2): p. 294-306.

77. Besson, M.T., L. Soustelle, and S. Birman, *Selective high-affinity transport of aspartate by a Drosophila homologue of the excitatory amino-acid transporters.* Curr Biol, 2000. **10**(4): p. 207-10.

78. Seal, R.P., et al., *Identification and characterization of a cDNA encoding a neuronal glutamate transporter from Drosophila melanogaster.* Receptors Channels, 1998. **6**(1): p. 51-64.

79. Rival, T., et al., *Decreasing glutamate buffering capacity triggers oxidative stress and neuropil degeneration in the Drosophila brain.* Curr Biol, 2004. **14**(7): p. 599-605.

80. Winter, N., P. Kovermann, and C. Fahlke, *A point mutation associated with episodic ataxia 6 increases glutamate transporter anion currents.* Brain, 2012. **135**: p. 3416-3425.

81. Huang, S. and R.J. Vandenberg, *Mutations in transmembrane domains 5 and 7 of the human excitatory amino acid transporter 1 affect the substrate-activated anion channel.* Biochemistry, 2007. **46**(34): p. 9685-92.

82. Stacey, S.M., et al., *Drosophila glial glutamate transporter Eaat1 is regulated by fringe-mediated notch signaling and is essential for larval locomotion.* J Neurosci, 2010. **30**(43): p. 14446-57.

83. Parinejad, N., et al., *Disruption of an EAAT-Mediated Chloride Channel in a Drosophila Model of Ataxia.* Journal of Neuroscience, 2016. **36**(29): p. 7640-7647.

84. van den Maagdenberg, A.M., et al., *A Cacna1a knockin migraine mouse model with increased susceptibility to cortical spreading depression.* Neuron, 2004. **41**(5): p. 701-10.

85. Eikermann-Haerter, K., et al., *Genetic and hormonal factors modulate spreading depression and transient hemiparesis in mouse models of familial hemiplegic migraine type 1.* J Clin Invest, 2009. **119**(1): p. 99-109.